Research Square

Preprints are preliminary reports that have not undergone peer review.
They should not be considered conclusive, used to inform clinical practice,
or referenced by the media as validated information.

Advanced Mitigation of Potato Virus Y Using Bentonite-Derived Nanoclay for Viral Suppression and Enhanced Plant Defense

MUHAMMAD BASEER US SALAM

muhammadbaseerussalam@gmail.com

https://orcid.org/0000-0002-6152-2879

AFIA ZIA

MUHAMMAD NAUMAN AHMAD

SHAH SAUD

Research Article

Keywords: Montmorillonite, Potato Virus Y (PVY), Bentonite-derived nanoclay, Antiviral activity, Oxidative stress, Sustainable agriculture

Posted Date: August 24th, 2026

DOI: https://doi.org/10.21203/rs.3.rs-10447408/v1

License: This work is licensed under a Creative Commons Attribution 4.0 International License. Read Full License

Abstract

Potato virus Y (PVY) is a major constraint on global potato production, causing yield losses of up to 83% in Pakistan. The current study was designed to assess the antiviral efficacy of bentonite-derived nanoclay obtained from selected alluvial deposits of the Attock–Cherat Range, Pakistan, namely, Chirat Dam Deposits (L1) and Jalozai Spring Deposits (L2) in mitigating PVY infection in potato plants. The nanoclay was characterized using Fourier Transform Infrared Spectroscopy (FTIR), X-ray Fluorescence (XRF), X-ray Diffraction (XRD), and Cation Exchange Capacity (CEC) analysis. Characterization confirmed typical bentonite structural features, including silicate functional groups, dominant oxides (SiO_2, Al_2O_3, Fe_2O_3), and montmorillonite as the predominant mineral phase. Under a factorial glasshouse experimentation, various applications methods i.e., foliar spray (F), soil amendment (S) and combined foliar–soil treatment (F + S) at concentrations of 1% – 3% was applied prior to viral inoculation. Pre-inoculation treatments were included to assess nanoclay as a potential defense-priming agent capable of activating antioxidant pathways prior to viral challenge. Disease severity, oxidative stress markers (malondialdehyde and hydrogen peroxide), antioxidant enzymes activities (peroxidase and polyphenol oxidase), and relative PVY accumulation, as determined by DAS-ELISA, was assessed. Nanoclay treatments significantly reduced PVY symptom severity and oxidative stress while enhancing antioxidant enzyme activities. The strongest suppression of disease was observed with combined foliar and soil application at 3% applied 48 hours before inoculation. The study demonstrated that bentonite-derived nanoclay significantly reduced PVY-associated disease severity, viral accumulation (DAS-ELISA), and oxidative stress while enhancing antioxidant defense responses under greenhouse conditions.

1. INTRODUCTION

Potato (*Solanum tuberosum* L.) is a globally important staple crop which significantly contribute to the global food security. However its productivity is severely affected by viral infections, particularly *Potato virus Y* (PVY), which is considered one of the most destructive. PVY alone is responsible for yield reduction of 20–40% worldwide with reported loss up to 83% in Pakistan (Solankey, 2025; Ahirwar & Pachaya, 2024). Potatoes are vulnerable to approximately 40 viruses and two viroids and mixed viral infections are common (Lai et al., 2022). Among these, *Potyvirus yituberosi* (potato virus Y, PVY) and *Potexvirus exiguum* (potato virus X, PVX) are the most prevalent in Pakistan, causing significant yield losses, while other viruses like *Potato Virus S* (PVS), *Potato Virus A* (PVA), *Potato Virus M* (PVM) and *Polerovirus solanacearum (potato leafroll virus, PLRV)* contribute to lower but still serious damage (Tessema et al., 2024; Kumar et al., 2022). Viral diseases have reduced potato yields in Pakistan by up to 83%, largely due to the use of uncertified, virus-infected seeds tubers and limited farmer awareness (Abbas et al., 2012). PVY is major global threat inducing symptoms like leaf yellowing, necrosis, leaf drop, and premature plant death (Kumar et al., 2022). It is an aphid-transmitted virus belonging to family *Potyviridae*, In agriculture, protection of crops from viral infection is considered to be a key priority. Conventional management focuses on controlling disease vectors through insecticides, natural predators, physical barriers, early sowing, crop rotation, and removal of infected plants (Abd El-Rahim et al., 2020). The current usage of nanoclay based materials has been widely used in various areas within agriculture; however, their antiviral activity has been limited (Aseel et al., 2022). The application of nanomaterials as soil amendment is attributed to the unique physico-chemical abilities of clay minerals including high adsorption capacity and cation exchange capacity which could increase soil fertility, assist in supplying nutrients to plants and help to build plant strengths (Margal et al., 2023; Ditta et al., 2015). Among these clay minerals, Bentonite is a sedimentary clay which is rich in montmorillonite mineral. It is derived from volcanic ash, offers these advantages and is well-suited for agricultural use (Haider et al., 2016). The incorporation of bentonite nanoclay into agricultural nanotechnology offers a eco-friendly and sustainable approach to manage plant health challenges. These are considered less toxic, environmental-friendly and cost-effective.

Studies on metallic, metal oxide, silica nanoparticles, and nanocomposites have shown high efficacy in delaying or suppressing pathogen effects, with reported reductions of 53%–84.5% in tomato and watermelon pathogens (Noman et al., 2023; Wang et al., 2022). However, data on nanoparticle efficacy against viral infections remain limited. Nanoclays, as layered silicate minerals, possess distinct physicochemical properties due to their 1:1 or 2:1 tetrahedral-octahedral sheet arrangements, influencing their applications (Abd-Elsalam et al., 2024; Singh et al., 2021; Majeed et al., 2013). With nearly 30 types identified (Savic et al., 2014), nanoclays' unique mineralogy underpins their potential in sustainable agriculture. Clay mineral nanotechnology is an emerging field offering eco-friendly materials that enhance crop production and reduce reliance on chemical fertilizers and pesticides. However, the antiviral efficacy of naturally derived nanoclay against plant pathogens as mitigation strategies is still unexplored.

Khyber Pakhtunkhwa province of Pakistan has large amounts of sedimentary clay deposits that contain Montmorillonite particularly in areas such as Dak Ismail Khel (District Nowshera), Karak, and Swat. These deposits were previously discussed as having the potential to supply Bentonite for various Industrial applications. The study of local communities in District Bannu revealed usage of clay from the River Kasho for day-to-day tasks, such as making detergents, body wash, pots and potter's clay, as well as to help heal wounds. There have been very few studies performed to establish the properties of this clay and to explore it potential uses. Bentonite has been identified in many sedimentary deposits in Pakistan through multiple studies (Rehman et al., 2021; Shah et al.,2013; Ahmad et al., 2011; Grim et al.,1978). Despite all these studies, many of these deposits, including those studied, have not been thoroughly identified, characterized for specific industrial uses, or analyzed for their microporous and mesoporous structure. The present research, to best of our knowledge is among the first attempts to

evaluate bentonite-derived nanoclay from indigenous deposits as a defense-priming agent against PVY infection in potato. The study further investigated the role of nanoclay in modulating oxidative stress and antioxidant defense mechanisms associated with plant resistance. Therefore, the present study aimed to isolate and comprehensively characterize bentonite-derived nanoclay from indigenous deposits of the Attock–Cherat Range, Pakistan, and evaluate its potential to mitigate Potato virus Y (PVY) infection in potato under greenhouse conditions. Specifically, the effects of nanoclay source, application method (foliar, soil, and combined), and concentration on disease severity, viral accumulation (DAS-ELISA), oxidative stress markers (malondialdehyde and hydrogen peroxide), and antioxidant enzyme activities (peroxidase and polyphenol oxidase) were investigated. The findings provide insight into the potential of naturally derived bentonite nanoclay as an environmentally sustainable strategy for enhancing plant defense against viral diseases.

2. MATERIALS AND METHODS

2.1. Soil Sampling and Nanoclay Preparation

Alluvial soil samples were collected from the Attock-Cherat Range (0–15 cm depth) using an auger, based on previous study of bentonite-rich mountains in the area Haider et al., (2016). Samples were air-dried at 40°C, sieved (2mm mesh) and chemically pretreated according to Kunze et al. (1989) to remove soluble salts, carbonates, and organic matter using distilled water, 0.5 M sodium acetate, and 30% H_2O_2, respectively. Following pretreatment, the finest clay particles (< 2 µm) were isolated via overnight sedimentation, and the supernatant was siphoned off. The isolated fine fraction was then oven-dried at 40°C for 72 hours. The dried clay was milled at 700 rpm for 3 hours to produce nanoclay, as described by Saleh et al. (2021). Standard bentonite (Sigma-Aldrich, CAS No: 1302-78-9) was processed similarly for comparison. The commercially available standard bentonite was included as a reference material to provide a benchmark for evaluating the physicochemical properties and biological performance of the locally sourced bentonite samples (L1 and L2). This comparison enabled assessment of whether indigenous bentonite deposits possess comparable antiviral potential.

2.2. Nanoclay's Characterization

Physico-chemical characterization of nanoclays isolated from selected bentonite-rich alluvial deposits were performed at the National Center of Excellence in Geology and Centralized Resource Laboratories, University of Peshawar, Pakistan. The systematic evaluation utilized a multi-facted approach in order to establish key morphological, structural and elemental characteristics of the samples. Key investigated parameters included:

2.2.1. Fourier Transform Infrared (FTIR)

Nanoclay samples were characterized using FTIR spectroscopy to identify their characteristic functional groups. The resulting vibrational nodes were then evaluated against those reported by Aseel et al., (2022), providing a useful reference to interpreting the structural and chemical properties.

2.2.2. X-Ray Fluorescence Spectrophotometer (XRF):

The elemental composition of the samples was determined by XRF spectrometry following the standard protocol outlined by Khalid *et al.*,2015. In order to ensure the analytical inconsistency and minimize the matrix effects, samples were subjected to drying, fine milling and homogenized. A comprehensive elemental profile was obtained covering major elements namely, Silicon (Si), Aluminum (Al), Iron (Fe), Magnesium (Mg), Calcium (Ca), Sodium (Na), Potassium (K), Zinc (Zn), Copper (Cu), Nickel (Ni), Lead (Pb) etc. were also analyzed using XRF.

2.2.3. X-Ray Diffraction (XRD):

Crystallographic analysis and phase identification were determined using a Rigaku ULTIMA IV Powder X-Ray Diffractometer with Cu-Kα radiation source (λ = 1.540598 Å. The system was operated at 20–60 kV with a maximum power output of 3 kW. The diffraction data was collected at ambient temperature across a 2θ range of 10°–90° employing goniometer radius of 285 mm and a minimal reduced step of 0.0001. The utilization of both Bragg-Brentano and parallel beam optics ensured high angular resolutions. The XRD patterns were obtained at room temperature in the range of 10–90, with basic accuracy (± 0.01°). A focal spot size of 0.4*12 mm was chosen to optimize the flux for accurate phase quantification.

2.2.4. Cation Ion Exchange (CEC):

CEC analysis was performed using modified standard protocol of Sumner and Miller (1996) and Ryan and Garabet (1994). Soil sample of approximately 4g of soil taken in a falcon tube. To this, 33 mL of 1N sodium acetate solution was added. After shaking for one hour and centrifuging at 3000 rpm for ten minutes, the supernatant was decanted. These processes were carried out four successive times. Subsequently, the soil residue was then washed with 33 mL of ethanol followed by centrifugation and the ethanol wash was then discarded. The diluted supernatant was analyzed for sodium, potassium, calcium, and magnesium using atomic absorption spectroscopy (AAS) against established calibration curves. Concentrations were converted to milliequivalents per 100 grams of soil, and the sum of these exchangeable

cations yielded the CEC of the soil sample. The primary elements of Calcium (Ca), Magnesium (Mg), Potassium (K), and Sodium (Na) were determined via this CEC analysis.

2.3. Experimental Design and Greenhouse Plantation

The current research employed a glasshouse experimentation using a full factorial CRD (Completely Randomized Design). The design comprised of two factors, namely foliar application and soil amendment. The treatments included applications of nanoclay derived from two different locations (Location 1; Chirat Dam and Location 2; Jalozai Spring) and standard bentonite (Procured from SIGMA ALDRICH). The treatments were applied via foliar spray, soil amendment and their combination. All treatments were applied at three different concentrations (1%, 2%, and 3%) pre-inoculation of the virus. Similarly, triplicates were used against each treatment. Data were collected weekly over a period of three weeks. Additionally, two controls (Negative and Positive) were taken. The negative control comprised of healthy potato plants that received no PVY inoculation or nanoclay treatment. The positive control consisted of PVY-inoculated plants that received no nanoclay treatment representing the baseline physiological condition. As these controls were not subjected to the factorial treatment structure, they were excluded from the statistical analysis and used solely as biological references for comparative interpretation.

“Pre-treatment” in the present study, refers to the application of nanoclay 48 hours prior to PVY inoculation. Treatments applications were conducted at the 30-day plant growth stage upon the expansion of two upper true leaves. The experimental treatments was classified into three primary application types names, foliar application (F), Soil Amendment (S) and combined foliar and soil application (FS). Each application strategy comprised of three nanoclay sources, namely, Chirat Dam Deposit (L1), Jalozai Natural Spring Deposits (L2) and Standard Bentonite (L3; Sigma Aldrich). It was evaluated across three selected concentrations (1% to 3%), resulting in nine treatment combinations per application method. Additionally, two control groups i.e., positive and negative controls were taken to ensure the experimental validity. The total number of experimental units (pots) was calculated based on the factorial arrangements of replicates, treatments, sources and concentrations which accounted for 249 units including controls ((3*3*3*3*3) + 6)). The present study evaluated selected nanoclay under various application methods for disease resistance in potato. Virus-free tubers of the potato variety *Desiree* were procured from the Barani Agricultural Research Station in Kohat, Pakistan for this glasshouse experiment, produced via meristem culture, ELISA indexed and officially certified as “Virus Free”. Virus-free tubers of the potato cultivar Désirée were used throughout the experiment. Désirée is a cultivar generally regarded as susceptible to Potato virus Y (PVY) and is therefore widely used in studies investigating PVY infection and disease management.

2.3.1. Experimental Trial, Plant Cultivation, and Viral Inoculation

The current research was carried out in the glasshouse facility at the Agricultural Research Farm (ARF), The University of Agriculture, Peshawar-Pakistan. Potato tubers were grown in 30 cm diameter plastic pots, each containing 4 kg of sterilized soil composed of an equal mixture of sand, field soil, and leaf compost (pH 7.2). All pots received a uniform basal dose of fertilizer to meet the nutritional requirements of potato crops. Plants were carefully maintained throughout the entire course of study, with regular monitoring of water conditions to prevent extremes of waterlogging or dryness. Additionally, insect repellents were deployed to mitigate infestations from pests such as aphids, ticks, and whiteflies. After 30 days of growth, two upper true leaves of each plant were marked and dusted with 600-mesh carborundum. A naturally infected potato leaf sample showing typical PVY symptoms was obtained from local potato fields and used as the inoculum source. The isolate was confirmed serologically as *Potato virus Y* (PVY) using a commercial DAS-ELISA kit prior to inoculation. No molecular strain typing (e.g., PVY^O, PVY^N, or PVY^NTN) was performed; therefore, the virus is referred to throughout this manuscript as *Potato virus Y* (PVY). Subsequently, mechanical inoculation was performed using the forefinger method. The inoculum was prepared at a 1:10 (w/v) ratio in 100 mM sodium phosphate buffer (pH 7.0) containing 0.5% 2-mercaptoethanol, following the protocol of Aseel et al. (2022). To minimize the effects of diurnal variation on oxidative stress markers and antioxidant enzyme activities, all leaf samples were collected at the same time of day under similar environmental conditions throughout the experiment. Leaf sampling was destructive. Independent sets of biological replicate plants were maintained for each weekly sampling interval (7, 14, and 21 days after inoculation). At each sampling time, young fully expanded leaves were collected from the designated plants for biochemical and serological analyses, after which the sampled plants were discarded and were not used for subsequent assessments.

2.3.2. Preparation of Enzyme Extract

Fresh leaf samples (100 mg) were homogenized in the appropriate extraction buffer according to the respective biochemical assay using a chilled mortar and pestle. The homogenates were centrifuged under the conditions specified for each assay, and the resulting supernatants were immediately collected and used as crude enzyme extracts for the determination of malondialdehyde (MDA), hydrogen peroxide (H_2O_2), peroxidase (POX), and polyphenol oxidase (PPO) activities. The composition of the extraction buffer and assay-specific conditions are described in the corresponding sections below.

2.4. Determination of Oxidative Stress Markers

2.4.1. Malondialdehyde (MDA)

Malondialdehyde (MDA) concentration of the leaf samples was determined using the procedure of Aseel et al. (2022). 100 mg of leaf samples were homogenized in 0.1% TCA, reacted with thiobarbituric acid (TBA) reagent followed by incubation at 95°C. Following centrifugation, the absorbance of the reaction mixture was measured spectrophotometrically at 532 nm and corrected for non-specific turbidity by subtracting the absorbance recorded at 600 nm. Malondialdehyde (MDA) concentration was calculated using the corrected absorbance ($A_{532} - A_{600}$) and the appropriate extinction coefficient. The resulting MDA-TBA complex measured were calculated against a standard curve illustrated in Fig. 4 prepared using 1,1,3,3-tetramethoxypropane-derived MDA.

2.4.2. Hydrogen Peroxide (H_2O_2)

In order to find the Hydrogen peroxide (H_2O_2) concentration, the protocol of Junglee et al. (2014) was followed. 100 mg of leaf tissue samples was homogenized in 0.1% TCA, centrifuged, and the supernatant reacted with 1M KI in 10 mM phosphate buffer (pH 7.0). After 20 min incubation at room temperature the absorbance was measured at 390 nm. The formula given for determining H2O2 is as:

$$H_2O_2\ (\mu\ \mathrm{mol/g}\ ) = \frac{\frac{\Delta A}{\in} * 1}{\mathrm{V} * 10^6} \sum \ldots\ldots\ldots 1$$

where ΔA refers to the variations in absorbance measured at 390 nm, ε = 0.28 μmol⁻¹ cm⁻¹ (extinction coefficient), l = 1cm (optical path length of the cuvette) and V indicates the total volume of the reaction mixture.

2.5. Evaluation of Antioxidant Enzymes Activity

2.5.1. Peroxidase (POX)

Peroxidase (POX) activity was determined according to the method of Angelini et al. (1990). Fresh leaf extract (1.2 mL) prepared in 100 mM phosphate buffer (pH 7.0) was mixed with 0.5 mL of 5 mM guaiacol and 120 µL hydrogen peroxide (H_2O_2). The reaction mixture was incubated at 30°C for 10 min, after which the absorbance was measured spectrophotometrically at 480 nm. Peroxidase activity was calculated using the change in absorbance relative to the blank and expressed according to the following equation:

$$POX\ Activity\ \left(\frac{U}{mL}\right) = \frac{\frac{\Delta A}{min}}{\in * l * V}\ \sum \ldots\ldots\ldots 2$$

where ΔA/min: Change in absorbance per minute at 480 nm, ∈: Extinction coefficient of the guaiacol oxidation product (26,600 $M^{-1}cm^{-1}$), l: Path length of the cuvette (usually 1 cm) V: Total volume of the reaction mixture (in milliliters). Guaiacol oxidation was monitored continuously by measuring the increase in absorbance at 480 nm throughout the reaction period, and POX activity was calculated from the change in absorbance per minute (ΔA/min). One unit (U) of peroxidase activity was defined as the amount of enzyme causing a change in absorbance of 0.001 per minute under the assay conditions.

2.5.2. Polyphenol Oxidase (PPO)

Polyphenol oxidase (PPO) activity was determined following Cho et al. (1999). Leaf extract (500 µL) in Tris buffer was mixed with 1 mL 50 mM catechol solution (in 100 mM Tris-HCl, pH 6.0). After 10 min incubation, absorbance was measured at 420 nm.

$$PPO\ Activity\ \left(\frac{U}{mL}\right) = \frac{\frac{\Delta A}{min}}{\in * l * V}\ \sum \ldots\ldots\ldots 3$$

where ΔA/min: Change in absorbance per minute at 420 nm, ∈: Extinction coefficient of the catechol oxidation product (1623 M-1 cm-1), l: Path length of the cuvette (usually 1 cm) V: Total volume of the reaction mixture (in milliliters). One unit (U) of polyphenol activity was defined as the amount of enzyme causing a change in absorbance of 0.001 per minute under the assay conditions.

2.5.3. Serological Detection and Severity Assessments

For the current study, the serological detection protocol of Clark and Adams, 1977 was followed by using double antibody sandwich (DAS) enzyme-linked immunosorbent assay (ELISA). DAS-ELISA was selected because it is a widely accepted and routinely employed serological technique for the detection and relative quantification of PVY in plant tissues. The method enabled consistent confirmation of viral infection across all treatments under identical experimental conditions. The DAS-ELISA Kit was procured from Bioreba AG, Switzerland along with following all the manufacturer's instructions. The serological detection and severity test was carried out at an interval of 7th, 14th and 21st day of the inoculation following Hameed et al., 2014. Relative PVY accumulation was assessed using a DAS-ELISA protocol. Leaf sap for ELISA was prepared from the two youngest fully expanded leaves of each plant to ensure uniform physiological age. Approximately 0.2 g of leaf tissue was homogenized in extraction buffer at a 1:10 (w/v) ratio, following the DAS-ELISA kit protocol, and this procedure was applied uniformly across all the samples. Purified polyclonal PVY antibodies were diluted in carbonate buffer (pH 9.6) and coated onto each well (200 µl/well), followed by 24 h incubation at 4°C. After three PBS-Tween washes, diluted leaf sap (200 µl/well, mixed with extraction buffer containing Tween-20, PVP-25, ovalbumin, and PBS) was added and incubated for 24 h at 4°C. Non-specific binding was prevented by a 30-minute incubation with BSA blocking

buffer at room temperature. Following three more PBS-Tween washes, plates were coated with conjugate antibody and incubated for 24 h at 4°C, then washed again. Finally, p-nitrophenyl phosphate substrate buffer was added to each well, and optical density was measured at 405 nm after 30 minutes in the dark. Triplicates of each sample, along with positive and negative controls, were used.

For severity test, the scoring method was followed as suggested by Islam et al., 2015. Table 1 depicts the severity rating table

Table 1
Scoring index and disease rating scale for Potato Virus Y's symptoms

Index	Reaction	PVY Symptoms
0	**Highly Resistant**	No visible symptoms
1	**Resistant**	Mild leaf vein chlorosis/ Blackening with initial mosaic patterns on leaves.
2	**Moderate Resistant**	Severe systemic vein blackening with leaf narrowing, veinal necrosis, severe mosaic and leaf crinkling.
3	**Moderate Susceptible**	Leaf rugosity, leaf drop steaking and plant dwarfing
4	**Susceptible**	Basal leaf senescence, plant wilting/collapse and reduced tuber development.

2.5.4. Statistical Analysis:

All experimental data were analyzed using Statistix 8.1 software (Analytical Software, Tallahassee, FL, USA). The experiment was conducted as a completely randomized design (CRD) with a three-factor factorial arrangement comprising application method, nanoclay concentration, and bentonite source, with sampling week included as a repeated temporal factor where applicable. ANOVA was performed to evaluate the main effects and interactions among the factorial treatment factors, and means were compared using Fisher's LSD test at $P < 0.05$. Data are presented as mean ± standard deviation (SD). Positive and negative controls were included to confirm PVY infection and establish healthy and infected baseline responses. Because these controls were not part of the factorial treatment structure, they were not included in the factorial ANOVA; instead, they were used as biological reference points for descriptive comparison with treated plants.

3. RESULTS AND DISCUSSIONS

3.1. Characterization of Bentonite Derived Clay:

3.1.1. Fourier Transform Infrared (FTIR) Spectroscopy Analysis:

The characteristic vibrational bands of functions groups for the selected samples are illustrated in Fig. 1. The findings represented the structural homology alongside the compositional heterogeneity as compared to the standard clay. The comparative evaluation provided an insight into the mineralogical composition alongside geogenic variation influencing the functional performance of the clay. The results were found align with Borah et al., 2022; Ali et al., 2022 and Kumar and Lingfa, 2020. Findings revealed that the structural framework is characterized by Si-O-Si bending at 417.46 cm^{-1} and Al-O-Si stretching at 525.55 cm^{-1} reflecting the intact primary silicate and aluminosilicate frameworks in bentonite (Kumar & Lingfa, 2020). Band at 627 cm^{-1} corresponded to Si-O stretch and indicated quartz impurities, while peaks at 755–786 cm^{-1} confirmed Al-containing silicates (Fletcher & Sposito, 1989). Spectral intensities analysis indicated that AS-01 and AS-02 had slightly reduced Si-O and Al-O intensities as compared to standard likely due to the differences in crystallinity (Khan et al., 2017; Shah et al., 2013). AS-02 exhibited a higher peak intensity which is an indication of high quality and purity. Similarly, the characteristic Si-O-Si and Al-O-Si peaks highlighted the silicate framework's role in improving soil structure. H-O-H bending and stretching peaks at 1636.3 and 3445 cm^{-1} confirmed water retention, enhancing soil and moisture regulation (Wali et al., 2023). Atmospheric CO_2 (O = C=O stretch at 2380 cm^{-1}) was noted as expected contamination (Jha, 2018). The functional groups Si–O–Si, Al–O–Si, and surface hydroxyl groups confirmed the characteristic physicochemical properties of bentonite, including its adsorption potential for a range of biological and chemical compounds. However, direct interactions between bentonite-derived nanoclay and plant viruses remain largely unexplored (Pan et al., 2023; Pardo et al., 2020; Zhao et al., 2012; Cuadros, 2017; Abdelkrim et al., 2020; Mansilla et al., 2020).

3.1.2. X-ray Fluorescence (XRF) Analysis

XRF analysis of alluvial soil samples AS-01 and AS-02 revealed a higher concentration of SiO_2 (58.66% and 61.96%) compared to the bentonite standard (55.07%), hence, identifying a greater presence of silicate or quartz minerals. The primary oxides identified and quantified include SiO_2, Al_2O_3, Fe_2O_3, CaO, and TiO_2. The higher SiO_2 level observed in AS-01 and AS-02 suggests an improved structural stability and potential suitability for construction use. The findings are in-line with the reported literature i.e., 61.7% (Ahonen et al. 2008, 49.87% (Kumar and Lingfa, 2020, 52.55% (Abdullahi and Audu, 2017, 55.55% (Alves et al. 2016) and up to 64.71% (Crespo et al., 2024). Likewise, the lower Al_2O_3 concentrations in AS-01 ((18.145%) and AS-02 (17.693%) relative to standard (26.087%) were found in-line with reported studies (Abdullahi & Audu, 2017; Crespo et al., 2024), further suggesting a regional variation affecting CEC. The reduced alumina level indicated a diminished nutrient-holding and swelling

capacity, potentially restricting the agricultural application unless amended (Kumar & Lingfa, 2020). However, high SiO_2 and moderate Al_2O_3 may still enhance soil structure and buffering. XRF results showed beneficial CaO levels (AS-01: 10.654%, AS-02: 8.989%), higher than the standard (3.192%), similar to Crespo et al. (2024), indicating potential in soil pH buffering and structural uses. Elevated K_2O (AS-01: 3.069%, AS-02: 3.042%) suggests feldspar/mica content, supporting plant nutrition (Kumar & Lingfa, 2020). Lower Fe_2O_3 (AS-01: 7.937%, AS-02: 7.084%) than the standard (11.082%) may affect fertility and pigmentation potential (Ahonen et al., 2008; Alves et al., 2016). TiO_2 was also lower in AS-01 and AS-02 compared to the standard (2.715%), implying reduced photocatalytic suitability (Alves et al., 2016).

Minor oxides like V_2O_5, MnO, and ZrO_2 were present in trace amounts, consistent with prior findings (Alves et al., 2016). Overall, the oxide abundance followed: SiO_2 > Al_2O_3 > Fe_2O_3 > CaO > K_2O > TiO_2 > MnO > V_2O_5 > SrO > ZrO_2, confirming silica dominance and potential for soil conditioning and structural applications. All the findings are presented in Table 2 (A) and Table 2 (B).

Table 2
(A): Oxides Analysis of the selected Samples by XRF

Oxides	Std Clay	AS-01	AS-02
SiO_2	55.07%	58.66%	61.96%
Al_2O_3	26.09%	18.15%	17.69%
Fe_2O_3	11.08%	7.94%	7.08%
CaO	3.19%	10.65%	8.99%
TiO_2	2.71%	0.91%	0.94%
K_2O	1.45%	3.07%	3.04%

Table 2
(B): Mineral Analysis (%) of Samples by XRF

Minerals	Bentonite Std.	AS-01	AS-02
Si	46.48	44.77	50.72
Al	21.42	14.93	14.63
Fe	19.65	15.02	13.03
Ca	5.27	17.464	14.63
Ti	3.72	1.39	1.38
K	2.65	5.5	5.47
Sr	0.17	0.075	0.09
vMn	0.14	0.286	0.17
V	0.12	0.05	0.059
Zr	0.1	0.065	0.09
Cr	0.08	0.06	0.03
Cu	0.06	0.04	0.04
Zn	0.04	0.04	0.03
Ni	0.02	0.02	0.01
Nb	0.01	-	-
Y	0.01	0.01	0.01
Rb	-	0.014	0.05

The predominance of SiO_2 and Al_2O_3 confirms the aluminosilicate nature of the bentonite-derived nanoclay, while the presence of Fe_2O_3, CaO, MgO, and K_2O reflects a mineral composition capable of influencing its cation exchange capacity and surface reactivity. These physicochemical characteristics may enhance the interaction of the nanoclay with the rhizosphere and plant surfaces, thereby improving nutrient retention and creating conditions favorable for enhanced physiological performance. Although the present study did not investigate

direct relationships between individual mineral constituents and antiviral activity, the observed reduction in disease severity and oxidative stress is consistent with the beneficial effects associated with montmorillonite-rich bentonite materials.

3.1.3. X-Ray Diffraction:

X-ray diffraction (XRD) analysis confirmed montmorillonite as dominate phase with characteristic peaks at 2θ = 5.22° and 34.2° consistent with the primary clay mineral in bentonite. Additionally, a peak at 11.6° indicated the presence of kaolinite, a mineral commonly found in bentonite, which may influence its adsorption properties due to kaolinite's relatively lower swelling capacity compared to montmorillonite.

The sharpness of the montmorillonite peaks suggests a relatively high crystallinity with values of Bentonite std. (99.37%), AS-01 (97.40%), and AS-02 (99.11%), reflecting high quality and purity. Illite peaks observed at 8.5° and 35° contributed to overall plasticity of the material but potentially influencing reactivity and swelling potential. Minor quartz impurities were detected at 20–25°, 26°, and 50° alongside weak feldspar at 27°.

Montmorillonite, owing to its high swelling capacity, cation exchange capacity, and surface area, may facilitate interactions with biological molecules and contribute to improved soil physicochemical properties. However, whether these properties directly influence PVY particles was not investigated in the present study (Lipson & Stotzky, 2019). Kaolinite also plays a role in adsorption through surface hydroxyls as well as enhancing soil structure (Duarte-Silva et al., 2014; Bhattacharyya and Gupta, 2008). Illite gives an effect to moderate adsorption and quartz improves porosity even though the reactivity is low (Li et al., 2019; Götze et al., 2021). Although Kaolinite was present in a low quantity, it lowers bentonite swelling and cation-exchange capacity. The findings were found consistent with prior comparisons of bentonite and kaolin clays (Kumar & Lingfa, 2020). The high crystallinity of the present samples further suggested a well-ordered structure favorable for adsorption and ion exchange, hence, supporting its agricultural utility. Although quartz and feldspar are subordinate phases, they may contribute to mechanical strength and thermal stability. Overall, these results accord with earlier reports on bentonite characterization and its broad applications in agriculture, water treatment, catalysis, and drug delivery (Alves et al., 2016; Ismaeel et al., 2017; Abdullahi & Audu, 2017; Erdoğan Alver et al., 2016; Ahmed et al., 2012; Ikhtiyarova et al., 2012; Asad et al., 2013; Berillo & Ermukhambetova, 2024; Rana & Kim, 2024; Verma et al., 2024).

3.1.4. Cation Exchange Capacity

In order to meaure the exchangeable cations, atomic absorption spectrophotometry (AAS) was used. Selected cations i.e., Ca++, Mg++, K + and Na + and their concentration (mg/L) was then transformed to milliequivalents of 100 grams of soil (meq/100g). All the findings are presented in Fig. 3. The net value recorded was 44.83 meq/100g and was found within the global varied range of bentonite and montmorillonite-rich soils (35 to 60 meq/100g) (Rengasamy and Olsson, 1991). Montmorillonite, which has a hypothetical CEC of over 100 meq/100g when pure (Oueslati and Meftah, 2026), is characterized by its high surface area, high density of charges and a layered structure. Calcium was found predominant i.e., (24.5 meq/100 g) corresponding to calcium-saturated bentonite deposits likely resulting from calcite dissolution as reported by Landon (2014). Magnesium followed at 16.7 meq/100g reflected smectite clay weathering and retention capacity (Sposito, 2008). Potassium (2.79 meq/100g) indicated fieldspar and mica fixation (Bell et al., 2020). Sodium was minimal, confirming the low salinity influence compared to sodium-dominated bentonites commonly found in arid regions (Churchman & Lowe, 2012). The presence of the calcium-dominated exchange complex indicates the calcareous property from Attock-Cherat deposits, depicting an improves potential as soil amendments. The presence of a good Ca:Mg ratio in the majority of samples is promising to maintain the soil structure and nutrient supply. Even though the level of sodium was low, its presence can still be dangerous under some circumstances by causing soil dispersion. Pretreatment with gypsum or organic matter might be necessary in such instances to reduce risks of sodicity (Rengasamy & Olsson, 1991).

Although the CEC plays a vital role in assessing the fertility of the soil and mineral interactions there are limited studies that focus on CEC in the characterization of bentonite. This is due of geological studies which tend to focus more on structural and industrial qualities rather than agronomic usefulness whereas CEC measurements are more prevalent in the field of soil science. Also, standardization is complicated by variability in CEC with differences in mineralogy, surface area and exchangeable ions. The available literature is based on sodium-containing bentonites, as they have salinity problems, so calcium- and magnesium-containing ones do not have enough literature representation in geology.

The high CEC and a favourable Ca:Mg ratio of the bentonites contributes to their suitability as soil conditioners, especially in arid and semi-arid soils where nutrient retention and soil structure are very vital. The concentrations of cations (in mg/L), their conversion to meq/100g and the total CEC values are shown in Fig. 3. These results support the agronomic and versatility of the bentonites of the Attock-Cherat range, which are consistent with the global literature on the montmorillonites-rich soils (Mejri and Oueslati, 2025; Sharma and Sharma, 2025; Ray et al., 2025).

The CEC values of L1, L2, and the commercially available standard bentonite were comparable, suggesting that all three materials possessed similar ion-exchange capacities. Therefore, the minor differences observed in biological performance are more likely associated with subtle variations in mineral composition or other physicochemical characteristics rather than differences in CEC alone.

3.2. Experimental Design and Green House Plantations

The findings of the study are as:

3.2.1. Determination of Oxidative Stress Markers:

Selected oxidative stress markers i.e., malondialdehyde (MDA) and hydrogen peroxide (H_2O_2) were quantified in order to evaluate the biochemical response of potato plants to PVY infection and nanoclay treatments. Leaf tissues were collected and homogenized in appropriate extraction buffers, followed by spectrophotometric analysis. The findings are as:

3.2.1.1. Malondialdehyde (MDA)

Malondialdehyde, a well-established indicator of membrane damage and lipid peroxidation under oxidative stress (Yekti et al., 2018), was quantified to assess the PVY-cellular injury alongside the mitigating impact of bentonite-derived nanoclay treatments. All the findings are presented in Tables 3,4 and 5. Statistical analysis confirmed a significant effect of Application method, nanoclay concentration, source, and sampling time (week) against MDA accumulation ($p < 0.001$). Likewise, significant interactions effects ($p < 0.001$) among application method, concentration, and source and sampling time indicated that MDA accumulation was jointly affected by treatment combinations and temporal progressions of infection while the three-way interaction (A×B×C) was not significant ($P > 0.05$; Table 5), suggesting an independent behaviour.

Mean comparison using LSD at (*$P \leq 0.05$) is* presented in Table 4 at the 5% significance level, with distinct letter groupings indicating statistically significant differences among treatments. The application type showed the strongest effect followed by concentration, while nanoclay source and temporal variation exhibited comparatively moderate contributions. A treatment-dependent relation in MDA accumulation was evident from the study. The highest MDA escalation was observed in the positive control increasing from 103 µmol g^{-1} FW to 314 µmol g^{-1} FW over a period of three weeks, depicting progressive oxidative damage attributed to viral replication and systemic infection. In contrast, the negative control exhibited the least MDA level depicting normal physiological conditions.

Among treatments, the combined application (F + S) consistently resulted in the lowest MDA levels (Table 4). In week 1, the MDA level ranged between 120–154 µmol g^{-1} FW, which further declined to 102–146 µmol g^{-1} FW (week 2) and reached 90–113 µmol g^{-1} FW by week 3, representing approximately 65–71% reduction in MDA at week 3 compared to the positive control (314 µmol g^{-1} FW), indicative of most effective mitigation of PVY-Induced oxidative damage. Compared to this, "Foliar Application" moderately reduced the oxidative stress from ~ 178–202 µmol g^{-1} FW (week 1) to ~ 101–148 µmol g^{-1} FW (week 3) corresponding to almost 40–55% reduction relative to control. Similarly, "Soil Amendment' exhibited the least efficacy from ~ 155–263 µmol g^{-1} FW (week 1) to ~ 154–173 µmol g^{-1} FW (week 3) corresponding to 30–45% reduction.

The results also revealed a concentration-responsive pattern (Table 4) across all weeks, where increasing concentrations (1% – 3%) significantly reduced MDA accumulation. The least MDA ((< 100 µmol g^{-1} FW) were observed at 3%, confirming optimal conditions and values approaching those of the negative control treatments, highlighting effective mitigation of oxidative damage. A minimal effect was observed for the "source" of the nanoclay, since standard bentonite exhibited lower MDA concentrations compared to L1 and L2 where intermediate responses were observed. The temporal dynamics for treated plants revealed a progressive decline from > 150 µmol g^{-1} FW (week 1) to < 100 µmol g^{-1} FW (week 3), representing a reduction in lipid peroxidation and an improved oxidative stability during infection progression. The nanoclay efficacy increased with infection progression as evident by highly significant treatment × time interaction ($P < 0.001$). A distinct difference between high-stress treatments (> 200 µmol g -1 FW) and optimized nanoclay treatments (< 100 µmol g -1 FW) was observed.

Observations from integrated applications revealed a decline in MDA levels (~ 90–98 µmol g^{-1} FW) to similar levels as non-infected plants (~ 76–88 µmol g -1 FW) suggesting that the oxidative balance and membrane integrity were restored nearly. Among the treatments, combined application types outperformed possible due to an improved distribution of nanoclay and enhanced interaction with plant tissues which can strengthen plant defense. This effect was enhanced by the increase in the nanoclay concentration that further supported a dose effect relationship of protection against the oxidative stress caused by viruses (Al-Mokadem et al., 2022). The resulting effect may be linked with the enhanced ROS scavenging and activation of plant defense pathways i.e., salicylic acid–mediated systemic acquired resistance (SAR) and jasmonic acid–mediated induced systemic resistance (ISR) (Rashad et al., 2024; Canwei et al., 2020; Choudhary & Johri, 2009; Choudhary et al., 2007). However, SAR and ISR were not evaluated in the current study.

As per the reported physiological studies, MDA levels in plant-virus interaction typically falls under ~ 80 to 250 µmol g^{-1} FW where values below 100 µmol g^{-1} FW indicate minimal oxidative injury and values above 200 µmol g^{-1} FW reflect severe membrane lipid peroxidation (Sahu et al., 2022). The data indicated a reduction in MDA from 207.79 to 90.82 µmol g^{-1} FW (Table 4) therefore represents a substantial shift from severe oxidative stress toward near-normal physiological conditions. Similar reductions in MDA levels following nanomaterial or clay-based treatments have been reported in previous plant stress studies, where nanostructured materials regulated the antioxidant activity and reduced lipid peroxidation under biotic and abiotic stress conditions. For example, several studies have demonstrated that clay-based nanomaterials can alleviate oxidative damage in virus-infected or pathogen-challenged plants by improving ROS scavenging and strengthening plant defense responses (Keke et al., 2025; Al-Khayri et al., 2023; Ray et al., 2023). The experimental evidence aligns with earlier reports demonstrating that nanomaterials can modulate oxidative stress responses in plants, while also highlighting the greater efficacy of combined application strategies

and higher nanoclay concentrations. These results suggest that bentonite-derived nanoclay represents a promising, environmentally sustainable approach for mitigating virus-induced oxidative damage and enhancing plant resilience.

Table 3

Malondialdehyde (MDA) content (μm g^{-1} FW) in potato plants as affected by application methods, nanoclay concentration, sources and temporal dynamics. Values are presented as (mean ± SD);. F = folia application typer, S = soil ammendment, F + S = combined applications; L1 = Locally sourced cl ay from Location 1 (Chirat Dam Deposits), L2; Location 2 (Jalozai Spring Deposits);; Std Clay = standard bentonite; Negative control represents non-infected plants, whereas positive control represents PVY-infected untreated plants

Week	Conc. (%)	L1F	L2F	Std Clay-F	L1S	L2S	Std Clay-F	L1FS	L2FS	Std Clay-FS	Control	
											Negative	Positive
1	1	202.43 ± 0.65	198.71 ± 1.32	178.81 ± 0.99	263.159 ± 1.42	209.179 ± 1.58	206.353 ± 1.05	154.703 ± 1.90	131.79 ± 1.43	120.66 ± 1.20	76.16 ± 0.14	103.36 ± 0.15
	2	164.52 ± 2.11	158.64 ± 1.32	155.98 ± 0.99	225.249 ± 1.85	258.323 ± 1.69	232.453 ± 1.15	154.67 ± 0.73	146.68 ± 1.19	125.16 ± 1.84		
	3	148.45 ± 1.39	146.74 ± 1.27	146.79 ± 0.93	209.179 ± 1.58	218.253 ± 1.78	209.623 ± 1.71	141.17 ± 1.99	124.75 ± 1.19	112.3 ± 1.52		
2	1	122.37 ± 0.73	120.51 ± 1.47	115.44 ± 0.94	200.433 ± 1.55	176.779 ± 1.81	167.953 ± 1.75	110.09 ± 1.93	106.1 ± 1.43	97.86 ± 1.21	81.09 ± 0.19	223.44 ± 0.20
	2	122.7 ± 2.10	112.78 ± 1.30	107.07 ± 0.96	183.099 ± 1.70	180.123 ± 1.76	169.083 ± 1.02	112.12 ± 0.71	102.94 ± 1.20	88.88 ± 1.20		
	3	116.05 ± 1.50	108.34 ± 1.38	101.28 ± 0.95	183.429 ± 1.59	172.393 ± 1.89	160.713 ± 1.80	110.47 ± 1.98	102.1 ± 1.18	85.65 ± 1.27		
3	1	116.39 ± 0.69	108.68 ± 1.35	101.28 ± 0.95	155.513 ± 1.64	171.249 ± 1.54	164.213 ± 1.75	81.49 ± 1.94	102.56 ± 1.45	96.45 ± 1.20	88.75 ± 0.19	314.00 ± 0.21
	2	112.88 ± 2.09	104.98 ± 1.28	101.27 ± 0.94	177.119 ± 1.06	168.293 ± 1.19	154.923 ± 0.92	106.33 ± 0.75	97.41 ± 1.18	81.02 ± 1.44		
	3	110.52 ± 1.44	104.6 ± 1.45	101.06 ± 0.99	173.609 ± 1.81	164.593 ± 1.47	154.913 ± 1.95	104.82 ± 2.02	96.52 ± 1.18	81.01 ± 1.71		

Table 4

Mean comparison of MDA content (μm g^{-1} FW) under different treatments. Values with different letters represents significance at $P < 0.05$ (LSD). F = folia application typer, S = soil ammendment, F + S = combined applications; L1 = Locally sourced clay from Location 1 (Chirat Dam Deposits), L2; Location 2 (Jalozai Spring Deposits);; Std Clay = standard bentonite; Negative control represents non-infected plants, whereas positive control represents PVY-infected untreated plants

Conc. (%)	L1F	L2F	Std Clay-F	L1S	L2S	Std Clay-F	L1FS	L2FS	Std Clay-FS
1	147.06^{h}	142.63^{i}	131.84^{j}	207.79^{a}	202.25^{b}	185.49^{d}	124.37^{k}	115.68^{no}	98.35^{q}
2	133.37^{j}	125.47^{k}	121.44^{l}	194.10^{c}	185.08^{c}	175.08^{f}	118.82^{lm}	107.79^{p}	92.99^{r}
3	125.01^{k}	119.89^{l}	116.57^{mn}	185.74^{d}	179.51^{e}	170.22^{d}	113.48^{o}	104.99^{p}	90.82^{r}

Table 5
Analysis of variance (ANOVA) for the effects of application method (A), nanoclay concentration (B), source (C), and sampling time (E) on malondialdehyde (MDA) content in potato plants under PVY infection. DF = degrees of freedom; SS = sum of squares; MS = mean square; F = F-statistic; P = probability level. Significant effects were considered at P < 0.05. Interaction terms represent combined effects of experimental factors

Source	DF	SS	MS	F	P
Application (A)	2	275433	137717	14730.1	***
Concentration (B)	2	11613	5806.35	621.04	***
Source (C)	2	14127	7063.27	755.48	***
A*B	4	1023	255.827	27.36	***
A*C	4	1227	306.821	32.82	***
B*C	4	393	98.1528	10.5	***
A*B*C	8	40	5.02553	0.54	0.823
Replicate (D)					
Error A*B*C*D		54	505	9.34933	
Week €		2	129398	64698.8	1416265
A*E	4	6399	1599.72	35018.1	***
B*E	4	10315	2578.84	56451.1	***
C*E	4	15	3.68515	80.67	***
A*B*E	8	987	123.33	2699.7	***
A*C*E	8	94	11.7881	258.04	***
B*C*E	8	778	97.2871	2129.63	***
A*B*C*E	16	154	9.59654	210.07	***
Error A*B*C*D*E		108	5	0.04568	
Total	242	452505			
Grand Mean		141.33			
CV(Applicati*Concentra*Source*Replicate)		2.16			
CV(Applicati*Concentra*Source*Replicate*Week)		0.15			

3.2.1.2. H_2O_2:

Hydrogen peroxide (H_2O_2), a key reactive oxygen species involved in oxidative stress and defense signaling, was quantified to evaluate the impact of PVY infection and nanoclay-mediated mitigation. The statistical analysis revealed significant effects ($P < 0.001$) of application method, concentration, source, and sampling time on H_2O_2 accumulation, along with significant interaction effects, indicating treatment-dependent and time-dependent responses. However, the interaction B×C and the three-way interaction A×B×C were not significant ($P > 0.05$), implying no interaction among concentration and source of nanoclay. Table 7 presents the mean comparison using LSD at 5% significant level alongside different letter grouping represents the significant differences among treatments. The findings demonstrated that application method exerted the strongest influence, followed by source and concentration, while temporal variation showed a pronounced but consistent effect across treatments.

A treatment-driven variation in H_2O_2 accumulation was evident. A gradual decline in H_2O_2 levels was observed in the positive control (5.38 to 4.74 µmol g^{-1} FW), implying a sustained but slightly moderated oxidative stress over time. In contrast, the lowest H2O2 levels (~ 0.83 to 0.45 µmol g^{-1} FW) in negative control ensured the normal physiological conditions with minimal oxidative stress. Among the treatments, the dual-mode application method (F + S) exhibited the highest mitigation effect as shown in Table 7. A fluctuating but overall decreasing trend in H_2O_2 levels was observed across treatment groups, reflecting dynamic regulation of ROS during infection progression. The H2O2 levels declined from 2.39–3.55 µmol g^{-1} FW (week 1), stabilized at 3.04–3.51 (week 2) and a further reduced to 2.80–3.34 (week 3).

The combined treatment strategy (F + S) demonstrated the most pronounced mitigation effect (Table 7). In week 1, H_2O_2 levels under combined treatments ranged approximately between 2.39–3.55 µmol g^{-1} FW, which further stabilized to ~ 3.51–3.04 µmol g^{-1} FW (week 2) and declined to

~ 3.34–2.80 µmol g^{-1} FW by week 3. This corresponds to almost 35–45% reduction relative to positive control depicting the ROS suppression effectively. “Foliar application” resulted in a progressive stabilization from 3.89–4.29 (week 1) to 3.29–3.99 (week 3) corresponding to a moderate reduction (20–30%). “Soil application” exhibited lower efficacy comparatively ranging from 3.35–4.29 (week 1) to 3.10–4.49 (week 3) corresponding to a reduction of 15–25%.

The results demonstrated a dose-dependent trend across all treatments as shown in Table 8, where an increasing concentration reduced H_2O_2 accumulation significantly. The optimal mitigation efficacy was observed at 3% (2.80–3.08 µmol g^{-1} FW), reflecting a considerable reduction from high-stress levels. The effect of nanoclay source was significant but less pronounced compared to application method; an intermediate effectiveness was observed compared to standard bentonite. The temporal dynamics revealed a declining trend and suggested an improved oxidative balance over a period of time. The progressive efficacy was underscored by the highly significant treatment × time interactions ($P < 0.001$). A clear distinction was observed between high-stress treatments (> 4.5 µmol g^{-1} FW) and optimized nanoclay treatments (< 3.0 µmol g^{-1} FW).

These results are attributed to an improved distribution alongside an enhanced interaction with plant tissues and synergistic effects at both foliar and rhizospheric levels. The reduction in H_2O_2 may be associated with improved ROS scavenging and possible restriction of viral activity due to the adsorption properties of nanoclay. Hydrogen peroxide (H_2O_2) plays a dual role as both a reactive oxygen species and a signaling molecule in plant defense, where excessive accumulation leads to oxidative damage while controlled levels contribute to stress signaling. Additionally, other contributors include salicylic acid-mediated systemic acquired resistance (SAR) and jasmonic acid-mediated induced systemic resistance (ISR) (Sun et al., 2024; Ji, et al., 2024; Shabbir et al., 2026; Gupta et al., 2025). The findings were compared and found to align with previous reports showing that nanomaterials and clay-based amendments enhance antioxidant defenses and suppress ROS accumulation under stress (Tortella et al., 2020; Mazurkova et al., 2010; Tripathi et al., 2017; Levina et al., 2016; Galdiero et al., 2011; Abdelkhalek, 2020; Cai et al., 2019)

Table 6

Hydrogen Peroxide (H_2O_2) content (µmol g^{-1} FW) in potato plants as affected by application methods, nanoclay concentration, sources and temporal dynamics. Values are presented as (mean ± SD);.F = folia application typer, S = soil ammendment, F + S = combined applications; L1 = Locally sourced clay from Location 1 (Chirat Dam Deposits), L2; Location 2 (Jalozai Spring Deposits);; Std Clay = standard bentonite; Negative control represents non-infected plants, whereas positive control represents PVY-infected untreated plants

Week	Conc. (%)	L1F	L2F	Std Clay-F	L1S	L2S	Std Clay-S	L1FS	L2FS	Std Clay-FS	Control	
											Positive	Negative
1	**1**	3.89 ± 0.1	4.29 ± 0.1	3.49 ± 0.1	3.84 ± 0.13	3.35 ± 0.08	3.56 ± 0.1	2.39 ± 0.1	3.55 ± 0.08	3.38 ± 0.13	5.38 ± 0.68	0.83 ± 0.05
	2	3.64 ± 0.12	3.69 ± 0.09	3.19 ± 0.1	3.67 ± 0.1	4.29 ± 0.1	3.43 ± 0.14	3.79 ± 0.09	3.67 ± 0.09	3.28 ± 0.12		
	3	3.29 ± 0.13	3.56 ± 0.09	2.99 ± 0.12	3.35 ± 0.08	3.69 ± 0.1	3.19 ± 0.1	3.8 ± 0.06	3.57 ± 0.14	3.1 ± 0.09		
2	**1**	5.39 ± 0.1	5.06 ± 0.13	4.61 ± 0.07	3.01 ± 0.1	4.88 ± 0.1	4.25 ± 0.1	2.92 ± 0.05	3.3 ± 0.07	3.1 ± 0.05	4.99 ± 0.80	0.74 ± 0.13
	2	5.02 ± 0.14	4.76 ± 0.1	4.09 ± 0.1	5.35 ± 0.14	5.09 ± 0.1	4.57 ± 0.12	3.51 ± 0.08	3.39 ± 0.05	3.04 ± 0.02		
	3	4.88 ± 0.1	4.25 ± 0.1	3.89 ± 0.1	5.09 ± 0.1	4.76 ± 0.1	4.09 ± 0.1	3.54 ± 0.04	3.19 ± 0.02	3 ± 0.02		
3	**1**	4.91 ± 0.09	4.66 ± 0.11	3.89 ± 0.1	3.88 ± 0.1	3.89 ± 0.1	4.01 ± 0.1	2.99 ± 0.02	3.1 ± 0.07	2.9 ± 0.05	4.74 ± 0.75	0.45 ± 0.05
	2	4.49 ± 0.1	4.29 ± 0.1	3.08 ± 0.11	4.89 ± 0.1	4.7 ± 0.09	3.89 ± 0.1	3.31 ± 0.08	3.19 ± 0.05	2.84 ± 0.02		
	3	3.89 ± 0.1	3.99 ± 0.11	2.39 ± 0.1	4.49 ± 0.1	4.29 ± 0.1	3.1 ± 0.09	3.34 ± 0.04	2.99 ± 0.02	2.8 ± 0.02		

Table 7
Mean comparison of Hydrogen Peroxide (H_2O_2) content (µmol g^{-1} FW) under different treatments. Values with different letters represents significance at P < 0.05 (LSD). F = folia application typer, S = soil ammendment, F + S = combined applications; L1 = Locally sourced clay from Location 1 (Chirat Dam Deposits), L2; Location 2 (Jalozai Spring Deposits);; Std Clay = standard bentonite; Negative control represents non-infected plants, whereas positive control represents PVY-infected untreated plants

Conc. (%)	L1F	L2F	Std Clay-F	L1S	L2S	Std Clay-F	L1FS	L2FS	Std Clay-FS
1	4.72^{a}	4.66^{a}	3.99^{c}	4.69^{a}	4.69^{a}	3.96^{c}	3.53^{d}	3.41^{def}	3.05^{hi}
2	4.38^{b}	4.24^{b}	3.45^{de}	4.41^{b}	4.2^{b}	3.45^{de}	3.55^{d}	3.25^{fg}	2.96^{hi}
3	4.01^{c}	3.93^{d}	3.08^{gh}	4.03^{c}	3.93^{c}	3.09^{gh}	3.31^{ef}	3.12^{gh}	2.90^{i}

Table 8
Analysis of variance (ANOVA) for the effects of application method (A), nanoclay concentration (B), source (C), and sampling time (E) on malondialdehyde (MDA) content in potato plants under PVY infection. DF = degrees of freedom; SS = sum of squares; MS = mean square; F = F-statistic; P = probability level. Significant effects were considered at P < 0.05. Interaction terms represent combined effects of experimental factors

Source	DF	SS	MS	F	P
Application (A)	2	36.377	18.1884	506.98	***
Concentration (B)	2	14.04	7.0199	195.67	***
Source (C)	2	25.82	12.9098	359.85	***
A*B	4	2.798	0.6996	19.5	***
A*C	4	2.373	0.5934	16.54	***
B*C	4	0.261	0.0654	1.82	0.138
A*B*C	8	0.174	0.0218	0.61	0.7678
Replicate (D)					
Error A*B*C*D	54	1.937	0.0359		
Week €	2	19.918	9.9589	5721.16	
A*E	4	16.08	4.02	2309.38	***
B*E	4	0.687	0.1718	98.68	***
C*E	4	3.202	0.8005	459.89	***
A*B*E	8	0.58	0.0725	41.63	***
A*C*E	8	2.304	0.288	165.47	***
B*C*E	8	0.763	0.0954	54.78	***
A*B*C*E	16	0.689	0.043	24.73	***
Error A*B*C*D*E		108	0.188	0.0017	
Total	242	128.191			
Grand Mean	3.7837				
CV(Applicati*Concentra*Source*Replicate) 5.01					
CV(Applicati*Concentra*Source*Replicate*Week) 1.1					

3.2.2. Determination of Antioxidant Enzymes

3.2.2.1. Polyphenol Oxidase (PPO):

The present study employed poly-phenol oxidase activity as a key indicator of phenolic metabolism and plant defense mechanism. Tables 9, 10 and 11 present all findings. A significant effect of application method (A), nanoclay concentration (B), source (C), and sampling time (week) (E) on PPO activity (P < 0.001) was observed. The findings showed that PPO was highly affected by both treatment combinations and the

progression of infection over time. Mean comparisons using LSD at the 5% significance level ($P \leq 0.05$) revealed clear and distinct differences among the treatment groups. The findings exhibited a distinct treatment-dependent pattern. A higher enzymatic activity for Positive control indicated the activation of phenolic metabolism related to defence in the response to viral infection. In contrast, the negative control, in contrast exhibited the lowest PPO activity, which is indicative of basal physiological conditions. The elevated PPO activity, a typical defence mechanism is associated with the oxidation of phenolic compounds into antimicrobial quinones that inhibit the pathogens.

The highest PPO activity was recorded for the combined application method as compared to foliar application and soil application which had relatively lower effect (Table 10). The high enzymatic activity is likely due to biochemical protection as opposed to cellular damage due to stress. These findings suggested that nanoclay not only relieves oxidative stress but also regulated the defense activation of the plant. It was evident that there was a dose-dependent pattern with all treatments with PPO activity increasing significantly with an increase in nanoclay concentrations (1% – 3%). The highest activity was measured at 3% indicating a high level of activation of the phenolic defense pathways and enhanced resistance capabilities. A minimal yet significant effect of nanoclay source was observed. Both the locally sourced nanoclay exhibited a moderate efficacy compared to standard bentonite. Similarly, temporal progression demonstrated a progressive rise in PPO activity, revealing a long-term activation of defence mechanisms throughout viral spread. The trend was further supported by a significant treatment x time interaction ($P < 0.001$) which implied a nanoclay-mediated defense responses increases with time.

The enhanced enzymatic activity may be associated with elevated phenolic oxidation, leading to quinone accumulation and cell wall reinforcement, thereby strengthening host defense responses against PVY infection. Additionally, nanoclay may indirectly stimulate defense signaling pathways, enhancing the synthesis of secondary metabolites involved in plant resistance. PPO activity during the plant-virus interaction increases rapidly due to plant's induced defense system. A coordinated defensive response covering both the biochemical protection and oxidative stress regulation was evident during the current study. This was further supported by a reduced MDA levels which eventually demonstrated the modulating phenolic metabolism and resistance to PVY infection.

Table 9

Polyphenol Oxidase (PPO) content (U g^{-1} FW) in potato plants as affected by application methods, nanoclay concentration, sources and temporal dynamics. Values are presented as (mean ± SD);.F = folia application typer, S = soil amendment, F + S = combined applications; L1 = Locally sourced clay from Location 1 (Chirat Dam Deposits), L2; Location 2 (Jalozai Spring Deposits);; Std Clay = standard bentonite; Negative control represents non-infected plants, whereas positive control represents PVY-infected untreated plants

Week	Conc. (%)	L1F	L2F	Std Clay-F	L1S	L2S	Std Clay-F	L1FS	L2FS	Std Clay-FS	Control	
											Negative	Positive
1	**1**	2.51 ± 0.05	1.28 ± 0.02	1.93 ± 0.07	2.03 ± 0.05	1.81 ± 0.07	1.75 ± 0.05	1.34 ± 0.07	1.8 ± 0.04	1.03 ± 0.06	0.81 ± 0.04	5.32 ± 0.73
	2	1.35 ± 0.02	1.44 ± 0.04	1.82 ± 0.05	2.3 ± 0.05	1.85 ± 0.06	1.77 ± 0.04	1.62 ± 0.05	1.06 ± 0.04	1.5 ± 0.04		
	3	1.94 ± 0.07	1.49 ± 0.07	1.34 ± 0.05	1.81 ± 0.07	1.86 ± 0.02	1.88 ± 0.07	1.88 ± 0.02	1.28 ± 0.05	1.39 ± 0.05		
2	**1**	1.96 ± 0.02	1.91 ± 0.03	1.15 ± 0.07	1.48 ± 0.04	2.08 ± 0.05	1.56 ± 0.04	1.73 ± 0.04	1.5 ± 0.03	1 ± 0.03	0.60 ± 0.04	5.01 ± 0.78
	2	1.53 ± 0.06	1.91 ± 0.03	1.03 ± 0.06	1.84 ± 0.05	1.85 ± 0.07	1.11 ± 0.05	1.31 ± 0.06	1.6 ± 0.03	1.04 ± 0.03		
	3	1.22 ± 0.02	1.04 ± 0.07	1.01 ± 0.03	1.36 ± 0.06	1.33 ± 0.04	1.48 ± 0.02	1.44 ± 0.06	0.91 ± 0.04	1.12 ± 0.02		
3	**1**	1.36 ± 0.07	1.71 ± 0.07	1.01 ± 0.03	1.7 ± 0.02	1.73 ± 0.05	1.45 ± 0.06	0.87 ± 0.02	1.51 ± 0.06	1.12 ± 0.02	0.38 ± 0.04	4.68 ± 0.83
	2	1.39 ± 0.04	1.91 ± 0.06	1.59 ± 0.06	2 ± 0.04	1.8 ± 0.02	1.11 ± 0.02	0.98 ± 0.07	0.9 ± 0.05	0.94 ± 0.06		
	3	1.2 ± 0.06	1.17 ± 0.03	1.1 ± 0.02	1.54 ± 0.05	1.17 ± 0.02	1.48 ± 0.05	1.21 ± 0.06	0.9 ± 0.03	1.53 ± 0.05		

Table 10
Mean comparison of Polyphenol Oxidase (PPO) content (U g^{-1} FW) under different treatments. Values with different letters represents significance at P < 0.05 (LSD). F = folia application typer, S = soil ammendment, F + S = combined applications; L1 = Locally sourced clay from Location 1 (Chirat Dam Deposits), L2; Location 2 (Jalozai Spring Deposits);; Std Clay = standard bentonite; Negative control represents non-infected plants, whereas positive control represents PVY-infected untreated plants

Conc. (%)	L1F	L2F	Std Clay-F	L1S	L2S	Std Clay-F	L1FS	L2FS	Std Clay-FS
1	1.94^{a}	1.63^{f}	1.36^{m}	1.95^{a}	1.83^{c}	1.33^{n}	1.30^{o}	1.15^{q}	1.16^{r}
2	1.42^{l}	1.75^{d}	1.48^{j}	1.73^{e}	1.45^{k}	1.61^{g}	1.51^{i}	1.03^{t}	1.34^{mn}
3	1.45^{k}	1.23^{p}	1.42^{l}	1.87^{b}	1.58^{h}	1.50^{i}	1.60^{gh}	1.05^{s}	1.33^{n}

Table 11
Analysis of variance (ANOVA) for the effects of application method (A), nanoclay concentration (B), source (C), and sampling time (E) on malondialdehyde (MDA) content in potato plants under PVY infection. DF = degrees of freedom; SS = sum of squares; MS = mean square; F = F-statistic; P = probability level. Significant effects were considered at P < 0.05. Interaction terms represent combined effects of experimental factors

Source	DF	SS	MS	F	P
Application (A)	2	5.8227	2.91135	311.62	***
Concentration (B)	2	0.20483	0.10241	10.96	***
Source (C)	2	3.0664	1.5332	164.11	***
A*B	4	1.19703	0.29926	32.03	***
A*C	4	1.28545	0.32136	34.4	***
B*C	4	1.69972	0.42493	45.48	***
A*B*C	8	1.85979	0.23247	24.88	***
Replicate (D)					
Error A*B*C*D	54	0.5045	0.00934		
Week (E)	2	4.4141	2.20705	4996.76	
A*E	4	0.12152	0.03038	68.78	***
B*E	4	0.65305	0.16326	369.63	***
C*E	4	1.65074	0.41269	934.32	***
A*B*E	8	2.64363	0.33045	748.15	***
A*C*E	8	1.47618	0.18452	417.76	***
B*C*E	8	2.07237	0.25905	586.48	***
A*B*C*E	16	3.40521	0.21283	481.84	***
Error A*B*C*D*E		108	0.0477	4.42E-04	
Total	242				
Grand Mean	1.4862				
CV(Applicati*Concentra*Source*Replicate) 6.5					
CV(Applicati*Concentra*Source*Replicate*Week) 1.41					

3.2.2.2. Peroxidase Activity (Units g^{-1} FW)

Peroxidase (POX) was determined to evaluate the mitigating capacity of nanoclay against PVY infection. POX is an important antioxidant enzyme involved in reactive oxygen species (ROS) scavenging and regulating plant defense responses. All the results are presented in Tables 12, 13 and 14. The statistical analysis revealed that application method (A), nanoclay concentration (B), source (C), and sampling time (week) (E) had a significant effect on POX activity (P < 0.001). Also, the interaction effects were significant (P < 0.001) as well, which indicated that POX activity was highly affected. Statistically significant differences were confirmed by LSD Mean comparison at 5% significance level (P ≤

0.05) as shown in Table 13. Nanoclay concentration, among all the treatment groups, depicted the highest efficacy followed by application method and sampling time. Similarly, nanoclay source also exhibited a minimal yet significant effect.

The findings revealed a clear treatment-dependent effect on POX activity. PVY-infected plants (positive control) resulted in an enhanced POX activity when compared to healthy plants highlighting the activation of antioxidant defense mechanisms under oxidative stress rather than damage itself Conversely, the negative control had the lowest POX activity, which is normal physiological conditions. This POX activity is a normal plant response to detoxify the excess H 2 O 2 and enhanced cellular enzymatic defense mechanisms during infection. A temporal increase in POX activity was observed across weeks under infected conditions, indicating sustained activation of defense mechanisms during infection progression.

The combined application outperformed other treatments and resulted in an elevated POX activity (Table 12). POX activity under combined treatments ranged from approximately 5.72–6.33 units (1%), 6.61–7.57 units (2%), and 8.03–9.06 units (3%). The increased POX activity alongside decreased H2O2 levels previously provided an effective insight towards ROS scavenging and better redox homeostasis in the presence of nanoclay treatments. This indicated an effective detoxification of ROS rather than stress-induced activation. Foliar application (F) exhibited in moderate improvement as POX activity was between 5.25–5.77 units (1%), 5.34–6.36 units (2%), and 6.29–7.51 units (3%), which is the partial activation of antioxidant defense.

The POX values in soil application (S) at 1% (5.99–6.19) to (9.18) at 3%, corresponding to a more intense stress-induced enzymatic reaction but a relatively low stress reduction ability than integrated application, were relatively higher. A consistent concentration-dependent trend was evident across the treatments as POX activity was significantly increased with the nanoclay levels (1–3%). The optimal response was observed at 3% where the enzymatic activity was at its peak indicating the balanced stimulation of antioxidant defense system rather than a stress-induced imbalance. This further suggests that higher concentration of nanoclay is responsible for an improved stress tolerance. Likewise, the “nanoclay source” revealed a minimal yet statistically significant effect compared to application method and concentration, with std. Bentonite producing a higher enzymatic activity than L1 and L2 which exhibit intermediate response. The sustained activation of defense system supported by the progressive enhancement across sampling time (temporal dynamics) as supported by highly significant treatment × time interactions ($P < 0.001$), corresponding to time-dependent changes in nanoclay efficacy.

Under the optimized condition, the elevated POX activity further suggested an improvement in redox balance and efficient ROS detoxification. The response is likely due to stimulation caused by nanoclay alongside immobilization of viral movement via adsorption effects. Similarly, the role of activation of defense signaling pathways i.e., salicylic acid responses as well cell wall lignification also play a pivotal role. The POX activity is generally increased during the defense response under plant-virus interactions. The regulated elevation in POX activity under nanoclay treatments indicated a shift toward controlled defense activation rather than excessive oxidative damage. This observation was supported by the simultaneous decline in MDA and H_2O_2 levels during the current study. The findings were found in-line with the dual role of POX in stress response and immunity as studied by (Passardi et al., 2005) where elevated levels signaled pathogen recognition and controlled downregulation maintained ROS homeostasis. The nanoclay-treated groups exhibited primed immunity, suggesting activation of induced systemic resistance mechanisms (Aseel et al., 2022). Compared to traditional inducers (Kuc et al., 1975), nanoclay enabled faster response kinetics and broader coverage via dual-route delivery. Its ability to sustain POX activity within a protective range supported oxidative signaling models that emphasized the role of balanced ROS-scavenging in effective immunity (Torres et al., 2002). The present investigation demonstrated significant difference in polyphenol oxidase (PPO) activity between plants treated with nanoclay and those infected with PVY. This highlighted the enzyme's dynamic function in stress response. Plant defenses were successfully stimulated by these treatments which also balanced the management of reactive oxygen species (ROS) without causing excessive oxidative damage. This is similar with the mechanisms of systemic acquired resistance (SAR). The necessity of synergistic treatment options for optimal stress reduction is highlighted by the intermediate PPO levels observed in post-inoculation and soil-only applications, which indicate less effective defense activation presumably due to delayed nanoclay uptake or translocation.

Although the present study focused on enzymatic antioxidant responses, non-enzymatic antioxidant metabolites such as total phenolics and flavonoids were not quantified. Future studies incorporating these biochemical parameters would provide a more comprehensive understanding of the antioxidant mechanisms associated with bentonite-derived nanoclay-mediated resistance against PVY.

The activities of POX and PPO were determined according to the published assay protocols and were expressed on the basis of identical fresh tissue amounts rather than total soluble protein content. Although normalization to protein content would facilitate comparison of enzyme-specific activities, all samples were processed using identical extraction procedures and equal quantities of fresh tissue, allowing valid relative comparisons among treatments within the present study. Future investigations should include protein quantification to enable normalization of enzyme activities and further strengthen biochemical interpretation.

Table 12

Polyphenol Oxidase (POX) content (U g^{-1} FW) in potato plants as affected by application methods, nanoclay concentration, sources and temporal dynamics. Values are presented as (mean ± SD);.F = folia application typer, S = soil ammendment, F + S = combined applications; L1 = Locally sourced clay from Location 1 (Chirat Dam Deposits), L2; Location 2 (Jalozai Spring Deposits);; Std Clay = standard bentonite; Negative control represents non-infected plants, whereas positive control represents PVY-infected untreated plants

Week	Conc. (%)	L1F	L2F	Std Clay-F	L1S	L2S	Std Clay-F	L1FS	L2FS	Std Clay-FS	Control	
											Negative	Positive
1	**1**	4.94 ± 0.03	5.33 ± 0.04	5.34 ± 0.03	5.38 ± 0.04	6.65 ± 0.01	5.65 ± 0.03	10.89 ± 0.01	7.41 ± 0.03	6.93 ± 0.02	2.78 ± 0.13	5.58 ± 0.15
	2	5.43 ± 0.02	4.53 ± 0.01	6.47 ± 0.03	6.29 ± 0.01	5.75 ± 0.03	5.57 ± 0.03	5.95 ± 0.03	4.71 ± 0.03	6.01 ± 0.01		
	3	6.47 ± 0.03	6.21 ± 0.01	6.41 ± 0.03	6.65 ± 0.01	5.76 ± 0.03	6.75 ± 0.03	6.15 ± 0.03	6.23 ± 0.03	7.01 ± 0.02		
2	**1**	4.98 ± 0.03	5.6 ± 0.01	5.48 ± 0.03	7.64 ± 0.02	8.69 ± 0.03	8.22 ± 0.03	7.05 ± 0.03	7.96 ± 0.03	7.98 ± 0.04	2.52 ± 0.07	5.80 ± 0.11
	2	6.52 ± 0.03	5.56 ± 0.02	5.75 ± 0.03	6.89 ± 0.01	5.56 ± 0.03	5.85 ± 0.02	6.63 ± 0.03	5.66 ± 0.02	6.24 ± 0.03		
	3	7.61 ± 0.02	5.93 ± 0.03	5.82 ± 0.03	8.22 ± 0.02	7.76 ± 0.03	7.54 ± 0.02	6.67 ± 0.03	6.7 ± 0.02	7.11 ± 0.03		
3	**1**	5.85 ± 0.02	6.41 ± 0.03	5.82 ± 0.03	9.01 ± 0.04	10.07 ± 0.03	10.24 ± 0.03	9.16 ± 0.03	9.55 ± 0.03	9.18 ± 0.01	2.43 ± 0.16	6.19 ± 0.13
	2	7.14 ± 0.02	5.95 ± 0.03	6.72 ± 0.02	6.18 ± 0.03	6.66 ± 0.03	7.18 ± 0.04	5.91 ± 0.03	6.8 ± 0.04	6.75 ± 0.03		
	3	8.46 ± 0.04	6.74 ± 0.03	8.21 ± 0.03	8.17 ± 0.03	7.53 ± 0.02	8.66 ± 0.01	7.4 ± 0.02	6.9 ± 0.01	8.61 ± 0.03		

Table 13

Mean comparison of POX content (U g^{-1} FW) under different treatments. Values with different letters represents significance at $P < 0.05$ (LSD). F = folia application typer, S = soil ammendment, F + S = combined applications; L1 = Locally sourced clay from Location 1 (Chirat Dam Deposits), L2; Location 2 (Jalozai Spring Deposits);; Std Clay = standard bentonite; Negative control represents non-infected plants, whereas positive control represents PVY-infected untreated plants

Conc. (%)	L1F	L2F	Std Clay-F	L1S	L2S	Std Clay-F	L1FS	L2FS	Std Clay-FS
1	5.25^{u}	5.77^{q}	5.54^{s}	6.15^{o}	5.99^{p}	6.19^{o}	6.16^{o}	5.72^{r}	6.33^{mn}
2	6.36^{m}	5.34^{t}	6.31^{mn}	7.56^{g}	7.01^{j}	7.65^{f}	6.74^{k}	6.61^{l}	7.57^{g}
3	7.51^{h}	6.29^{n}	7.42^{i}	8.47^{c}	8.03^{e}	9.18^{a}	8.30^{d}	8.03^{e}	9.06^{b}

Table 14
Analysis of variance (ANOVA) for the effects of application method (A), nanoclay concentration (B), source (C), and sampling time (E) on malondialdehyde (MDA) content in potato plants under PVY infection. DF = degrees of freedom; SS = sum of squares; MS = mean square; F = F-statistic; P = probability level. Significant effects were considered at P < 0.05. Interaction terms represent combined effects of experimental factors

Source	DF	SS	MS	F	P
Application (A)	2	62.454	31.2269	10968.7	***
Concentration (B)	2	185.549	92.7743	32587.7	***
Source (C)	2	20.984	10.4919	3685.37	***
A*B	4	8.474	2.1185	744.13	***
A*C	4	2.006	0.5014	176.12	***
B*C	4	6.383	1.5958	560.55	***
A*B*C	8	6.289	0.7861	276.12	***
Replicate (D)					
Error A*B*C*D	54	0.154	0.0028		
Week €	2	112.332	56.1659	321515	***
A*E	4	9.722	2.4304	13912.5	***
B*E	4	21.45	5.3626	30697.3	***
C*E	4	2.706	0.6765	3872.62	***
A*B*E	8	7.338	0.9172	5250.5	***
A*C*E	8	5.134	0.6417	3673.56	***
B*C*E	8	6.582	0.8228	4710.09	***
A*B*C*E	16	10.011	0.6257	3581.74	***
Error A*B*C*D*E (F)	108	0.019	0.0002	108	
Total	242	467.585			
Grand Mean	6.9129				
CV(Applicati*Concentra*Source*Replicate) 0.77					
CV(Applicati*Concentra*Source*Replicate*Week) 0.19					

3.2.3. Serological Detection and Severity Assessments

3.2.3.1. ELISA

Serological assessment was carried out using DAS-ELISA to determine the relative accumulation of PVY based on ELISA absorbance values. The obtained ELISA absorbance values were used as a semi-quantitative indicator of relative PVY accumulation within host plant tissues. All the results are shown in Tables 15, 16 and 17. The statistical analysis revealed a highly significant effect of application method (A), concentration (B), source (C), and sampling week (E) on ELISA absorbance values ($P < 0.001$). Similarly, all the interaction effects were highly significant ($P < 0.001$) implying that virus accumulation is strongly influenced by the treatment method, treatment concentration, type of nanoclay and progression of infection through time. Comparisons of mean levels via the LSD test at 5% level of significance ($P \leq 0.05$) indicated distinct groups among the treatments. Application method was shown to have the most influential effect, while other factors included source and concentration, in addition to time which was consistently significant among all the treatments.

Among treatments, a pronounced variation trend in ELISA absorbance was observed. For the controls, the positive control had higher absorbance value with increasing levels from 4.74 (week 1) to 5.48 (week 2) and 5.82 (week 3). These values confirmed the presence of PVY infection and relatively higher viral antigen accumulation in the untreated infected plants. The negative control did not have any detectable signal (ND) implying that it was without any infection or rather in its normal physiology condition. Samples were considered positive upon their absorbance values exceedingly at least two to three times than negative control to ensure a reliable difference between infected and healthy plants.

The highest efficacy, among treatments were observed for combined application method (F + S). The ELISA values ranged within 1.77–2.71 (week 1), 1.79–3.09 (week 2), and 1.84–2.94 (week 3) depending on the source and concentrations used, representing approximately 45% to 65% compared to the positive control. Comparatively to untreated infected plants (> 5.0 absorbance units), the treated samples had significantly lower absorbance (< 3.0), indicating lower relative PVY accumulation compared with the untreated infected control. Unlike foliar application (F), which exhibited moderate effectiveness based on ELISA values ranging between 2.5–3.64, 2.25–2.90, and 1.48–2.96 across weeks respectively, corresponding to approximately 30–50% decrease compared to the positive control; Soil application (S) exhibited a relatively low effectiveness, having ELISA values of approximately 3.8–3.95 (week 1), 2.89–4.12 (week 2), and 3.23–3.95 (week3) correspondingly, equivalent to only 20–35% decrease.

A significant dose-dependent relationship was also observed, with 3% concentration resulting in the lowest viral titers (ELISA absorbance = 1.73–2.80), indicating enhanced mitigation efficacy. The effect was significant but less influential than application method and concentration. The standard bentonite clay generally exhibited slightly lower ELISA absorbance compared to L1 and L2, while the latter showed intermediate responses. Although both locally sourced bentonite samples exhibited comparable biological performance, slight differences in disease suppression and antioxidant responses were observed between L1 and L2. The CEC values of L1, L2, and the standard bentonite were comparable, indicating similar ion-exchange capacities. Therefore, the observed biological differences are more likely associated with subtle variations in mineral composition, as indicated by the XRF and XRD analyses, or other unmeasured physicochemical properties. However, particle size distribution was not determined in the present study; therefore, its contribution to the observed biological differences could not be evaluated.

Temporal behaviour revealed a progressive increase in ELISA values in untreated plants, whereas treated plants showed a comparatively stabilized or slightly declining trend across weeks, reflecting sustained suppression of viral accumulation. This trend was further supported by highly significant treatment × time interactions ($P < 0.001$) demonstrating that nanoclay efficacy becomes more pronounced with infection progression. The lowest values of ELISA was attributed with the declining trend of oxidative stress biomarkers namely, MDA, H2O2 and a consistent increase in anti-oxidant enzymes activities (POX and PPO). This corresponded to an integral linking response between viral suppression and an improved host defense.

The observed decline in viral accumulation may be associated with enhanced plant defense responses induced by nanoclay treatment, thereby limiting viral spread and disease development. However, the precise mechanism underlying this response was not investigated in the present study. During the plant–virus interactions, ELISA absorbance values typically increase due to active viral replication inside the host tissues. The reduction observed for the current study reflected an effective suppression of PVY infection and restoration toward near-normal physiological conditions.

The present findings demonstrate that nanoclay treatment significantly reduced PVY-associated disease severity and DAS-ELISA absorbance while enhancing antioxidant defense responses. However, the underlying mechanism of disease suppression remains unresolved. (Tripathi et al., 2017; Elbeshehy et al., 2015; Jain, 2014). The response aligned with zinc oxide nanoparticles ZnONPs/ SiO_2NPs- mediated immunity Cai *et al.*,2019; Elbeshehy *et al.*,, 2015 but exhibits a lower oxidative stress (MDA, H2O2) than metallic NPs (Tortella et al., 2020). Nanoclay is considered as scalable as compared to the complex green synthesis methods outlined by Abdelkhalek et al., 2020). The study determined an enhanced systemic protection against a combined foliar-soil at 48 hrs pre-inoculaton which was found in-line with (Durán et al., 2016; Galdiero et al., 2011), with sustained SAR similar to SiO_2NPs (Cai et al., 2019) depicting a greater efficacy. This approach has the potential to overcome the phytotoxicity–efficacy trade-off (Levina et al., 2016) and oxidative damage issues (Mazurkova et al., 2010).

Table 15

ELISA content (OD405nm) in potato plants as affected by application methods, nanoclay concentration, sources and temporal dynamics. Values are presented as (mean ± SD);.F = folia application typer, S = soil ammendment, F + S = combined applications; L1 = Locally sourced clay from Location 1 (Chirat Dam Deposits), L2; Location 2 (Jalozai Spring Deposits);; Std Clay = standard bentonite; Negative control represents non-infected plants, whereas positive control represents PVY-infected untreated plants

Week	Conc. (%)	L1F	L2F	Std Clay-F	L1S	L2S	Std Clay-F	L1FS	L2FS	Std Clay-FS	Control	
											Negative	Positive
1	**1**	2.5 ± 0.03	3.64 ± 0.03	3.09 ± 0.04	3.8 ± 0.03	3.95 ± 0.03	2.56 ± 0.03	2.67 ± 0.02	2.71 ± 0.01	1.77 ± 0.03	ND.	4.74 ± 0.06
	2	2.9 ± 0.02	2.32 ± 0.02	2.9 ± 0.01	3.8 ± 0.03	2.94 ± 0.03	3.38 ± 0.02	1.8 ± 0.04	2.81 ± 0.02	2.59 ± 0.03		
	3	2.96 ± 0.03	2.36 ± 0.02	2.96 ± 0.01	3.95 ± 0.03	3.31 ± 0.03	3.61 ± 0.03	2.96 ± 0.01	1.66 ± 0.03	2.68 ± 0.03		
2	**1**	2.39 ± 0.02	2.69 ± 0.03	3.31 ± 0.03	3.17 ± 0.03	3.75 ± 0.04	3.06 ± 0.02	1.79 ± 0.03	2.28 ± 0.02	2.92 ± 0.02	ND	5.48 ± 0.10
	2	2.25 ± 0.03	2.59 ± 0.03	2.51 ± 0.03	4.12 ± 0.02	2.89 ± 0.01	2.29 ± 0.03	2.03 ± 0.03	2.96 ± 0.03	3.09 ± 0.02		
	3	3.02 ± 0.03	1.48 ± 0.03	2.82 ± 0.01	3.32 ± 0.02	2.5 ± 0.01	3.15 ± 0.03	2.05 ± 0.03	2.49 ± 0.03	2.17 ± 0.04		
3	**1**	3.47 ± 0.03	2.2 ± 0.02	2.82 ± 0.01	2.41 ± 0.03	2.93 ± 0.03	3.1 ± 0.03	2.14 ± 0.01	1.84 ± 0.03	1.97 ± 0.03	ND	5.82 ± 0.07
	2	2.89 ± 0.03	1.85 ± 0.04	1.59 ± 0.02	3.66 ± 0.03	2.58 ± 0.03	2.09 ± 0.03	1.83 ± 0.01	2.34 ± 0.03	1.92 ± 0.03		
	3	1.73 ± 0.02	2.69 ± 0.01	1.99 ± 0.03	3.34 ± 0.03	3.23 ± 0.02	2.95 ± 0.02	2.94 ± 0.02	1.97 ± 0.03	2.8 ± 0.03		

Table 16

Mean comparison of MDA content (µmol g^{-1} FW) under different treatments. Values with different letters represents significance at P < 0.05 (LSD). F = folia application typer, S = soil ammendment, F + S = combined applications; L1 = Locally sourced clay from Location 1 (Chirat Dam Deposits), L2; Location 2 (Jalozai Spring Deposits);; Std Clay = standard bentonite; Negative control represents non-infected plants, whereas positive control represents PVY-infected untreated plants

Conc. (%)	L1F	L2F	Std Clay-F	L1S	L2S	Std Clay-F	L1FS	L2FS	Std Clay-FS
1	2.79^{ij}	2.84h	3.07e	3.86^{a}	2.80^{hi}	2.59^{m}	1.88^{t}	2.70^{k}	2.53^{n}
2	2.67kl	2.24pq	2.33o	3.48^{c}	3.01^{f}	3.23^{d}	2.65^{l}	2.04^{s}	2.55^{mn}
3	2.57mn	2.17r	2.36o	3.54^{b}	2.90^{g}	2.75^{j}	2.27^{p}	2.22^{qr}	2.18^{r}

Table 17
Analysis of variance (ANOVA) for the effects of application method (A), nanoclay concentration (B), source (C), and sampling time (E) on malondialdehyde (MDA) content in potato plants under PVY infection. DF = degrees of freedom; SS = sum of squares; MS = mean square; F = F-statistic; P = probability level. Significant effects were considered at P < 0.05. Interaction terms represent combined effects of experimental factors

Source	DF	SS	MS	F	P
Application (A)	2	27.1503	13.5751	4916.18	***
Concentration (B)	2	2.2065	1.1033	399.54	***
Source (C)	2	4.226	2.113	765.21	***
A*B	4	3.5167	0.8792	318.39	***
A*C	4	7.0656	1.7664	639.7	***
B*C	4	1.7462	0.4365	158.09	***
A*B*C	8	6.7752	0.8469	306.7	***
Replicate (D)					
Error A*B*C*D	54	0.1491	0.0028		
Week (E)	2	4.5001	2.25	16104.8	***
A*E	4	2.5509	0.6377	4564.53	***
B*E	4	1.1028	0.2757	1973.32	***
C*E	4	1.3234	0.3308	2368.08	***
A*B*E	8	2.9019	0.3627	2596.31	***
A*C*E	8	5.9692	0.7461	5340.63	***
B*C*E	8	10.1211	1.2651	9055.34	***
A*B*C*E	16	8.3679	0.523	3743.35	***
Error A*B*C*D	108	0.0151	0.0001		

3.2.3.2. Disease Severity Index

The present study aimed to assess the disease severity at regular week interval using a standardized rating scale. Statistical analysis revealed that disease severity was significantly affected (P < 0.001) by application method, nanoclay concentration, source, and sampling time.

The highest severity was observed in the positive control who exhibited the mosaic and vein banding at week 1, progressing to severe rugosity and dwarfing by week 3. Negative control, in contrast, plants remained healthy throughout the experimental study. The integrated application method (F + S) resulted in the least severity across weeks which confirmed the strong suppression of viral replication. Foliar application exhibited a moderate diseases suppression while soil amendment depicted least efficacy. The study revealed a clear concentration-dependent response with 3% nanoclay treatment consistently hindering the severity scores, followed by 2% and 1%. Minutes differences were observed among nanoclay sources, The standard clay source predominantly exhibited efficacy than local sources namely L1 and L2.

Table 18

Disease Severity Index in potato plants as affected by application methods, nanoclay concentration, sources and temporal dynamics. Values are presented as (mean ± SD);.F = folia application typer, S = soil ammendment, F + S = combined applications; L1 = Locally sourced clay from Location 1 (Chirat Dam Deposits), L2; Location 2 (Jalozai Spring Deposits);; Std Clay = standard bentonite; Negative control represents non-infected plants, whereas positive control represents PVY-infected untreated plants

Week	Conc. (%)	L1F	L2F	Std Clay-F	L1S	L2S	Std Clay-F	L1FS	L2FS	Std Clay-FS	Control	
											Negative	Positive
1	**1**	3.5 ± 0.5	2 ± 0.82	1.67 ± 1.25	3 ± 2.16	4 ± 0.82	2.33 ± 0.47	1.67 ± 1.25	1 ± 0.82	0.67 ± 0.47	0	3
	2	3 ± 0.82	2 ± 0.82	2 ± 0.82	4 ± 0.82	3.33 ± 0.47	2.67 ± 1.25	2 ± 0.82	0.33 ± 0.47	0.67 ± 0.47		
	3	2.33 ± 0.47	1.33 ± 0.47	1.33 ± 0.47	4 ± 0.82	3 ± 0.82	3 ± 0.82	1.33 ± 0.47	0.67 ± 0.47	0.67 ± 0.47		
2	**1**	2.33 ± 1.7	2 ± 0.82	1.67 ± 1.25	2.33 ± 0.47	3 ± 0.82	2 ± 0.82	0.67 ± 0.47	1 ± 0.82	0.67 ± 0.47	0	4
	2	3 ± 0.82	2 ± 0.82	1.33 ± 0.47	3.33 ± 1.7	3 ± 0.82	2.67 ± 1.25	2 ± 0.82	0.33 ± 0.47	0.67 ± 0.47		
	3	2.33 ± 0.47	1.33 ± 0.47	1.67 ± 1.25	3.33 ± 0.47	2.33 ± 0.47	1.67 ± 0.47	1.33 ± 0.47	0.67 ± 0.47	0.67 ± 0.47		
3	**1**	2.33 ± 1.7	2 ± 0.82	1.67 ± 1.25	1.67 ± 1.25	3 ± 0.82	2 ± 0.82	0.67 ± 0.47	0.67 ± 0.47	0.67 ± 0.47	0	5
	2	3 ± 0.82	1.33 ± 0.47	1.33 ± 0.47	2.67 ± 1.25	2.33 ± 0.47	2 ± 0.82	1.33 ± 0.47	0.67 ± 0.47	0.67 ± 0.47		
	3	2.33 ± 0.47	1 ± 0.82	1 ± 0.82	3 ± 0.82	2 ± 0.82	1.33 ± 0.47	0.33 ± 0.47	0.67 ± 0.47	0.67 ± 0.47		

Table 19

Mean comparison of MDA content (µmol g^{-1} FW) under different treatments. Values with different letters represents significance at $P < 0.05$ (LSD). F = folia application typer, S = soil ammendment, F + S = combined applications; L1 = Locally sourced clay from Location 1 (Chirat Dam Deposits), L2; Location 2 (Jalozai Spring Deposits);; Std Clay = standard bentonite; Negative control represents non-infected plants, whereas positive control represents PVY-infected untreated plants

Conc. (%)	L1F	L2F	Std Clay-F	L1S	L2S	Std Clay-F	L1FS	L2FS	Std Clay-FS
1	3^{abc}	3^{abc}	2^{bcdef}	3.67^{a}	3.33^{ab}	3.33^{ab}	1.67^{cdef}	0.89^{ef}	0.89^{ef}
2	2^{bcdef}	1.67^{cdef}	1^{ef}	2.67^{abcd}	2.33^{abcde}	2^{bcdef}	0.67^{f}	0.67^{f}	0.67^{f}
3	2^{bcdef}	1.33^{def}	1^{ef}	2.67^{abcd}	1.67^{cdef}	2^{bcdef}	0.67^{f}	0.67^{f}	0.67^{f}

Table 20
Analysis of variance (ANOVA) for the effects of application method (A), nanoclay concentration (B), source (C), and sampling time (E) on malondialdehyde (MDA) content in potato plants under PVY infection. DF = degrees of freedom; SS = sum of squares; MS = mean square; F = F-statistic; P = probability level. Significant effects were considered at P < 0.05. Interaction terms represent combined effects of experimental factors

Source	DF	SS	MS	F	P
Application (A)	2	132.971	66.4856	27.24	***
Concentration (B)	2	15.169	7.5844	3.11	0.0528
Source (C)	2	49.934	24.9671	10.23	***
A*B	4	5.597	1.3992	0.57	0.6831
A*C	4	6.461	1.6152	0.66	0.6212
B*C	4	1.3	0.3251	0.13	0.9695
A*B*C	8	4.23	0.5288	0.22	0.9866
Replicate (D)					
Error A*B*C*D	54	131.778	2.4403		
Week (E)	2	7.564	3.7819	114.87	***
A*E	4	4.609	1.1523	35	***
B*E	4	3.745	0.9362	28.44	***
C*E	4	0.535	0.1337	4.06	0.0042
A*B*E	8	4.23	0.5288	16.06	***
A*C*E	8	1.811	0.2263	6.88	***
B*C*E	8	2.082	0.2603	7.91	***
A*B*C*E	16	1.868	0.1168	3.55	***
Error A*B*C*D*E (F)	108	3.556	0.0329		
Total	242	377.44			
Grand Mean	1.781				
CV(Applicati*Concentra*Source*Replicate) 87.67					
CV(Applicati*Concentra*Source*Replicate*Week) 10.18					

4. CONCLUSION AND RECOMMENDATIONS

The current research demonstrated the potential of bentonite-derived nanoclay as an eco-friendly and sustainable source for mitigating the Potato virus Y (PVY) infection in potato plants. Mineralogical analysis confirmed the montmorillonite-dominated nanoclay with desirable physicochemical characteristics suitable for agriculture. Nanoclay treatments under greenhouse conditions exhibited reduction in oxidative stress markers (H_2O_2 and MDA), antioxidant enzyme activities (PPO and POX) and relative PVY accumulation, as indicated by DAS-ELISA absorbance. The severity assessment exhibited a significantly reduced symptom expression compared to healthy plants. Combined foliar and soil treatment, among the application methods, showed the highest efficacy alongside higher concentration (3%). The findings indicated that nanoclay inhibits the PVY development effectively by regulating the oxidative balance in plants and improving their defense mechanisms. These results demonstrate the potential of bentonite-based nanomaterials as environmentally-friendly antiviral agents to enhance crop health and develop nano-based plant protection protocols.

The current study recommends conducting long-term field trials as they are essential to validate nanoclay's effectiveness under diverse environmental conditions and agricultural practices, while also assessing its sustainability, impact on soil health and cost-effectiveness for commercial applications. Similarly, further studies are needed to elucidate the precise molecular and biochemical mechanisms by which nanoclay suppress the viral infection and enhances plant defense responses.

Limitation of the study:

The present study has several limitations. Morphological characterization (SEM/TEM), particle surface charge (zeta potential), and molecular confirmation of PVY by RT-PCR/qRT-PCR were not performed and should be incorporated in future investigations. Similarly, defense-related gene expression and non-enzymatic antioxidants (e.g., total phenolics and flavonoids) were beyond the scope of this work but would provide valuable mechanistic insights into nanoclay-induced resistance. In addition, a mock-inoculated control was not included; therefore, the potential contribution of mechanical inoculation to the observed physiological responses cannot be completely excludeds. Future studies should address these aspects to further elucidate the antiviral mechanisms of bentonite-derived nanoclay..

Declarations

Ethical Approval:

Not applicable.

Conflicts of Interest:

The authors declare no conflict of interest.

Funding:

This research work received no funding.

Author Contributions:

Conceptualization Muhammad Baseer Us Salam; **Methodology**, Afia Zia; **Software and Validation: Shahsaud**; **Formal analysis**: Muhammad Nauman Ahmad; **Write-up**: Muhammad Baseer Us Salam

Availability of data and materials:

All the data generated in this research work has been included in the manuscript.

References

1. Abbas MF, Hameed S, Rauf A, Nosheen Q, Ghani A, Qadir A, Zakia S (2012) Incidence of six viruses in potato growing areas of Pakistan. Pakistan J Phytopathol 24(3):44–47
2. Abd El-Rahim WMH, Moawad MM, Hashem GMM, Gebreil M, Zakaria (2020) Highly efficient fungal pectinase and laccase producers among isolates from flax retting liquor. Biocatal Agric Biotechnol 25(1):570–581
3. Abdelkhalek A, Al-Askar AA, Behiry SI (2020) Bacillus licheniformis strain POT1 mediated polyphenol biosynthetic pathways genes activation and systemic resistance in potato plants against Alfalfa mosaic virus. Sci Rep 10(1):16120
4. Abdelkhalek A, Hafez AE (2020) Plant Viral Diseases in Egypt and Their Control. Cottage Industry of Biocontrol Agents and Their Applications. Springer, Berlin/Heidelberg, Germany, pp 403–421
5. Abd-Elsalam KA, Mehmood MA, Ashfaq M, Abdelkhalek TE, Hassan RK, Ravichandran M (2024) Liquid Nanoclay: Synthesis and Applications to Transform an Arid Desert into Fertile Land. Soil Syst 8(3):73–84
6. Abdullahi SL and A.A. Audu.2017. Comparative analysis on chemical composition of bentonite clays obtained from Ashaka and tango deposits in Gombe State. Nigeria ChemSearch J, 8(2): 35–40
7. Ahmad SS, Barbhuiya A, Elahi A (2011) Effect of Pakistani bentonite on properties of mortar and concrete. Clay Miner 46(1):85–92
8. Ahmed AI, Yadav DR, Lee YS (2016) Applications of nickel nanoparticles for control of Fusarium wilt on lettuce and tomato. Int J Innovative Res Sci Eng Technol 5(5):7378–7385
9. Aseel DG, Abdelkhalek A, Alotibi FO, Samy MA, Al-Askar AA, Arishi AA, Hafez EE (2022) Foliar application of nanoclay promotes potato (Solanum tuberosum L.) growth and induces systemic resistance against potato virus Y. Viruses 14(10):2151–2159
10. Clark MF, Adams AW (1977) Characteristics of the microplate method of enzyme-linked immunosorbent assay (ELISA) for detection of plant viruses. Joural Gen Virol 34(3):475–483
11. Ditta A, Arshad M, Ibrahim M (2015) Nanoparticles in sustainable agricultural crop production: applications and perspectives Chap. 6. In: M.H. Siddiqui Nanotechnology and plant sciences: nanoparticles and their impact on plants, vol 10. Springer International Publishing Switzerland, pp 55–75

12. Liu DJB, Zhao T, Xu X, Lin H, Ji Y, Ding X (2022) Silica nanoparticles protect rice against biotic and abiotic stresses. J Nanobiotechnol 20(1):197–204
13. Grim RE, Guven N (1978) Bentonites—Geology, Mineralogy. Properties and Uses. Developments in Sedimentology. Elsevier, New York, USA
14. Hameed A, Iqbal Z, Asad S, Mansoor S (2014) Detection of multiple potato viruses in the field suggests synergistic interactions among potato viruses in Pakistan. Plant Pathol J 30(4):407–415
15. Islam MU, Muhammad S, Shahbaz M, Javed MA, Khan NH, Amrao L (2015) Screening of potato germplasm against RNA viruses and their identification through ELISA. J Green Physiol Genet Genome 1(1):22–31
16. Khalid N, Mukri M, Kamarudin F, Abdul Ghani AH, Arshad MF, Sidek N, Bilong B (2015) Effect of Nanoclay in Soft Soil Stabilization. In In InCIEC 2014: Proceedings of the International Civil and Infrastructure Engineering Conference. 905–914
17. Lai X, Wang H, Wu C, Zheng W, Leng J, Zhang Y, Yan L (2022) Comparison of potato viromes between introduced and indigenous varieties. Front Microbiol 13(3):809–815
18. Majeed. KM, Jawaid A, Hassan AA, Bakar HA, Khalil A, Salema I, Inuwa (2013) Potential materials for food packaging from nanoclay/natural fibres filled hybrid composites. Mater Designs 46(1):391–410
19. Margal PB, Gaikwad AS, Kamble BM, Titirmare NS (2023) Clay Mineral Nanotechnology: Innovation in Agriculture. Acta Sci Agric 7(11):229–235
20. Memon SA, Arsalan R, Khan S, Lo TY (2012) Utilization of Pakistani bentonite as partial replacement of cement in concrete. Constr Build Mater 30(3):237–242
21. Rehman MU, Manan A, Uzair M, Khan AS, Ullah A, Ahmad AS, Khan MA (2021) Physicochemical characterization of Pakistani clay for adsorption of methylene blue: Kinetic, isotherm and thermodynamic study. Mater Chem Phys 269:124722
22. Ryan J, Garabet S (1994) Soil test standardization in west Asia-North Africa Region. Commun Soil Sci Plant Anal 25(9–10):1641–1653
23. Saleh EMFM, Kishk RMR, Hedia AA, El-Shafei A, El-Latif M, Mona (2021) Efficacy of Nano-Clay Derived from Egyptian Alluvial Soils for Cu (II) Removal from Aqueous Solutions. Alexandria Sci Exch J 42(2):365–380
24. Savic I, Stojiljkovic S, Savic I D. Gajic. Industrial application of clays and clay minerals. In Clays and Clay Minerals: Geological Origin, Mechanical Properties and Industrial Applications; Wesley LR (ed); Nova Science: Hauppauge, NY, USA, 379–402
25. Farooq SLAM, Carvalho FM, da Silva Valenzuela MDG, Valenzuela FR, Díaz FR (2018) Investigation of mineralogy and porosity of two Pakistani bentonites and its corresponding purified bentonites. Arab J Sci Eng 43(1):373–382
26. A. SL, Khattak NS, Valenzuela M, Manan A, Díaz FV (2013) Preparation and characterization of purified Na-activated bentonite from Karak (Pakistan) for pharmaceutical use. Clay Miner 48(4):595–603
27. Shah. LAMG, Silva-Valenzuela AM, Ehsan FR, VelanzualaDiaz NS, Khattak (2013) Characterization of Pakistani purified bentonite suitable for possible pharmaceutical application. Appl Clay Sci 50(2):83–84
28. Singh H, Sharma A, Bhardwaj SK, Arya SK, Bhardwaj N, Khatri M (2021) Recent advances in the applications of nano-agrochemicals for sustainable agricultural development. Environ Science: Processes Impacts 23(2):213–239
29. Sumner ME, Miller WP (1996) Cation exchange capacity and exchange coefficients. Methods of soil analysis: Part 3 Chemical methods. 5. 1201–1229
30. Khan K, Khan SA, Saleem MU, Ashraf M (2017) Improvement of locally available raw bentonite for use as drilling mud. Open Constr Building Technol J, 11(1)
31. Shah LA, da Silva Valenzuela MDG, Ehsan AM, Díaz FRV, Khattak NS (2013) Characterization of Pakistani purified bentonite suitable for possible pharmaceutical application. Appl Clay Sci 83:50–55
32. Jha AK (2018) Bentonite for chemical industries. J J Indian Chem Soc 95:35
33. Abdelkrim S, Mokhtar A, Djelad A, Bennabi F, Souna A, Bengueddach A, Sassi M (2020) Chitosan/Ag-bentonite nanocomposites: preparation, characterization, swelling and biological properties. J Inorg Organomet Polym Mater 30:831–840
34. Wali S, Khattak MI, Khattak MI, Sjjad A (2023) Synthesis, Characterization and Application of Karak Bentonite Clay-Graft-Poly (Acrylamide/Co-Acrylic Acid) Superabsorbent Composite and its Adsorption Study for Selected Heavy Metals. J Chem Soc Pak, 45(3)
35. Verma S, Jha AK, Kumari P (2024) Studies on removal of Pb (II) by modified bentonite. Int J Chem Biochem Sci 25(14):548–552
36. Kumar A, Lingfa P (2020) Sodium bentonite and kaolin clays: Comparative study on their FT-IR, XRF, and XRD. Materials Today: Proceedings, 22, 737–742
37. Fletcher P, Sposito G (1989) The chemical modelling of clay/electrolyte interactions for montmorillonite. Clay Miner 24(2):375–391
38. Crespo E, Martín DA, Costafreda JL (2024) Bentonite Clays Related to Volcanosedimentary Formations in Southeastern Spain: Mineralogical, Chemical and Pozzolanic Characteristics. Minerals 14(8):814
39. Ahonen L, Korkeakoski P, Tiljander M, Kivikoski H, Laaksonen R (2008) Quality assurance of the bentonite material (No. POSIVA-WR–08–33). Posiva Oy

40. Alves JL, Zanini AE, Souza MD, Nascimento MLF (2016) Study of selection and purification of Brazilian bentonite clay by elutriation: a XRF, SEM and Rietveld analysis. Cerâmica 62(361):1–8
41. James OO, Adediran MM, Adekola FA, Odebunmi EO, Adekeye JID (2008) Beneficiation and characterisation of a bentonite from North-Eastern Nigeria. J N C Acad Sci 124(4):154–158
42. Trauger RL (1994) The structure properties, and analysis of bentonite in geosynthetic clay liners. Geosynthetic resins, formulation, and manufacturing, Proceedings of 8th GRI Conference
43. Holtzer M, Bobrowski A, Grabowska B (2011) Montmorillonite: a comparison of methods for its determination in foundry bentonites. Metab 50(2):119–122
44. Vingas GJ, Zrimsek AH (1964) Thermal stability of bentonites in foundry molding sand, in: Proceedings of the 13th National Conference on Clays and Clay Minerals, pp. 367–380
45. Asad AK, Shantanu AD, Mohammad H, Raquibul (2013) Suitability of bentonite clay: an analytical approach. Int J Earth Sci 2(3):88–95
46. Ahmed AS, Salahudeen N, Ajinomoh CS, Hamza H, Ohikere A (2012) Studies on the mineral and chemical characteristics of Pindiga Bentonitic Clay, Petrol. Technol. Dev. J. 1 1–8 (ISSN 1595–9104). An International Journal
47. Rana MS, Kim S (2024) Bentonite in Korea: A Resource and Research Focus for Biomedical and Cosmetic Industries. Materials, 17(9), 1982
48. Berillo D, Ermukhambetova A (2024) The review of oral adsorbents and their properties. Adsorption 30(6):1505–1527
49. Kunze GW, Dixon JB (1989) Pretreatment for Mineralogical Analysis, Methods of Soil Analysis, Part 1—Physical and Mineralogical Methods, 2nd edn. Agronomy Society of America and Soil Science of America. Wisconsin. 1181
50. Erdoğan Alver B, Alver Ö, Günal A, Dikmen G (2016) Effects of hydrochloric acid treatment on structure characteristics and C 2 H 4 adsorption capacities of Ünye bentonite from Turkey: a combined FT-IR, XRD, XRF, TG/DTA and MAS NMR study. Adsorption 22:287–296
51. Ismaeel SH, Mabrouk MS, Ali AAA, Elwalead KA (2017) Synthesis and characterization of bentonite nanocomposites from Egyptian bentonitic clay. Int J Nanatechnol Allied Sci 1(1):16–29
52. Ali HMZ, Zubair lrfan, M., Akbar G (2022) Analogize studies on the geochemistry of bentonite clays of Shaheed Ghat formation (early Eocene) from Eastern Sulaiman Range, Pakistan. Pakistan J Sci Industrial Res Ser A: Phys Sci 65(2):135–139
53. Shah LA, da Silva Valenzuela MDG, Ehsan AM, Díaz FRV, Khattak NS (2013) Characterization of Pakistani purified bentonite suitable for possible pharmaceutical application. Appl Clay Sci 83:50–55
54. Mansilla AY, Salcedo MF, Colman SL, Chevalier MT, Lanfranconi MR, Alvarez VA, Casalongué CA (2020) Characterization of functionalized bentonite as nanocarrier of salicylic acid with protective action against Pseudomonas syringae in tomato plants. Eur J Plant Pathol 158:211–222
55. Jha AK (2018) Bentonite for chemical industries. J J Indian Chem Soc 95:35
56. Abdelkrim S, Mokhtar A, Djelad A, Bennabi F, Souna A, Bengueddach A, Sassi M (2020) Chitosan/Ag-bentonite nanocomposites: preparation, characterization, swelling and biological properties. J Inorg Organomet Polym Mater 30:831–840
57. Verma S, Jha AK, Kumari P (2024) Studies on removal of Pb (II) by modified bentonite. Int J Chem Biochem Sci 25(14):548–552
58. Wahab N, Saeed M, Ibrahim M, Munir A, Saleem M, Zahra M, Waseem A (2019) Synthesis, characterization, and applications of silk/bentonite clay composite for heavy metal removal from aqueous solution. Front Chem 7:654
59. Haider N, Khan S, Ali A, Ali L (2016) Mineralogical and geochemical study of bentonite deposits of Garhi Chandan area, District Nowshera, Khyber Pakhtunkhwa, Pakistan. Arab J Geosci 9:1–10
60. Liu L (2013) Prediction of swelling pressures of different types of bentonite in dilute solutions. Colloids Surf A 434:303–318
61. Ikhtiyarova GA, Özcan AS, Gök Ö, Özcan A (2012) Characterization of natural-and organobentonite by XRD, SEM, FT-IR and thermal analysis techniques and its adsorption behaviour in aqueous solutions. Clay Miner 47(1):31–44
62. Churchman GJ, Lowe DJ (2012) Alteration, formation, and occurrence of minerals in soils. CRC, pp 1–72
63. Grim RE (1968) Clay Mineralogy: 2nd Edn McGraw-Hill. New York
64. Landon JR (2014) Booker tropical soil manual: a handbook for soil survey and agricultural land evaluation in the tropics and subtropics. Routledge
65. Borah D, Nath H, Saikia H (2022) Modification of bentonite clay & its applications: A review. Rev Inorg Chem 42(3):265–282
66. Mazurkova NA, Spitsyna Y, Shikina N, Ismagilov Z, Zagrebelny S, Ryabchikova E (2010) Interaction of titanium dioxide nanoparticles with influenza virus. Nanotechnol Russ 5:417–420
67. Levina AS, Repkova MN, Bessudnova EV, Filippova EI, Mazurkova NA, Zarytova VF (2016) High antiviral effect of TiO2 ·PL-DNA nanocomposites targeted to conservative regions of (–)RNA and (+)RNA of influenza A virus in cell culture. Beilstein J Nanotechnol 7:1166–1173 [CrossRef] [PubMed]
68. Galdiero S, Falanga A, Vitiello M, Cantisani M, Marra V, Galdiero M (2011) Silver nanoparticles as potential antiviral agents. Molecules 16:8894–8918

69. Cai L, Liu C, Fan G, Liu C, Sun X (2019) Preventing viral disease by ZnONPs through directly deactivating TMV and activating the plant immunity in Nicotiana benthamiana. Environ Sci Nano
70. Rengasamy P, Olsson KA (1991) Sodicity and soil structure. Soil Res 29(6):935–952
71. Tortella GR, Rubilar O, Diez MC, Padrão J, Zille A, Pieretti J, Seabra AB (2020) Advanced Material Against Human (Including Covid-19) and Plant Viruses: Nanoparticles as a Feasible Strategy. Glob Chall. 2000049. [Google Scholar] [CrossRef]
72. Durán N, Durán M, Jesus MB, Seabra AB, Favaro WJ, Nakazato G (2016) Silver Nanoparticles: A New View on Mechanistic Aspects on Antimicrobial Activity. Nanomedicine 12:789–799 [Google Scholar] [CrossRef]
73. Elbeshehy EK, Elazzazy AM, Aggelis G (2015) Silver nanoparticles synthesis mediated by new isolates of Bacillus spp., nanoparticle characterization and their activity against Bean Yellow Mosaic Virus and human pathogens. Front Microbiol 6:453
74. Jain D, Kothari S (2014) Green synthesis of silver nanoparticles and their application in plant virus inhibition. J Mycol plant pathol 44(1):21–24
75. Tripathi DK et al (2017) An overview on manufactured nanoparticles in plants: uptake, translocation, accumulation and phytotoxicity, Plant Physiol. Biochem 110:2–12
76. Naikoo GA, Mustaqeem M, Hassan IU, Awan T, Arshad F, Salim H, Qurashi A (2021) Bioinspired and green synthesis of nanoparticles from plant extracts with antiviral and antimicrobial properties: A critical review. J Saudi Chem Soc 25(9):101304
77. Sahu, P. K., Jayalakshmi, K., Tilgam, J., Gupta, A., Nagaraju, Y., Kumar, A., … Rajawat,M. V. S. (2022). ROS generated from biotic stress: Effects on plants and alleviation by endophytic microbes. Frontiers in Plant Science, 13, 1042936.
78. Rashad YM, Hafez M, Bourouah M, Abd-Elgawad AM, El-Sharkawy HH (2024) Montmorillonite nanoclay triggers immunity responses in wheat against Puccinia striiformis f. sp. tritici, and suppresses uredospore germination. Phytopathologia Mediterranea 63(2):269–281
79. Canwei S, Xiaoyun H, Ahmed N, Shiqi W, Erxun Z, Meide L (2020) Fructosan form Paenibacillus kribbensis PS04 enhance disease resistance against Rhizoctonia solani and tobacco mosaic virus. Electron J Biotechnol 47:43–50
80. Götze J, Pan Y, Müller A (2021) Mineralogy and mineral chemistry of quartz: A review. Mineral Mag 85(5):639–664
81. Li GL, Zhou CH, Fiore S, Yu WH (2019) Interactions between microorganisms and clay minerals: New insights and broader applications. Appl Clay Sci 177:91–113
82. Duarte-Silva R, Villa-García MA, Rendueles M, Díaz M (2014) Structural, textural and protein adsorption properties of kaolinite and surface modified kaolinite adsorbents. Appl Clay Sci 90:73–80
83. Bhattacharyya KG, Gupta SS (2008) Adsorption of a few heavy metals on natural and modified kaolinite and montmorillonite: a review. Adv Colloid Interface Sci 140(2):114–131
84. Pan Y, Zhang X, Ji C, Zhan Q, Li Z, Guan J, Huang J (2023) Modification method of high-efficiency organic bentonite for drilling fluids: a review. Molecules 28(23):7866
85. Pardo L, Domínguez-Maqueda M, Cecilia JA, Pozo Rodríguez M, Osajima J, Moriñigo MÁ, Franco F (2020) Adsorption of salmonella in clay minerals and clay-based materials. Minerals 10(2):130
86. Zhao W, Liu X, Huang Q, Walker SL, Cai P (2012) Interactions of pathogens Escherichia coli and Streptococcus suis with clay minerals. Appl Clay Sci 69:37–42
87. Cuadros J (2017) Clay minerals interaction with microorganisms: a review. Clay Miner 52(2):235–261
88. Lipson SM, Stotzky G (2019) Interactions between viruses and clay minerals. Human Viruses In Sediments Sludges & Soils. CRC, pp 197–223
89. Bañuelos, J. L., Borguet, E., Brown Jr, G. E., Cygan, R. T., DeYoreo, J. J., Dove,P. M., … Zhang, H. (2023). Oxide–and silicate–water interfaces and their roles in technology and the environment. Chemical Reviews, 123(10), 6413–6544.
90. Alexander JA, Ahmad Zaini MA, Surajudeen A, Aliyu ENU, Omeiza AU (2019) Surface modification of low-cost bentonite adsorbents—A review. Part Sci Technol 37(5):538–535
91. Yekti R, Bukhari A, Jafar N, Thaha AR (2018) Measurement of malondialdehyde (MDA) as a good indicator of lipid peroxidation. Int J Allied Med Sci Clin Res (IJAMSCR) 6(4):1–3
92. Al-Khayri, J. M., Rashmi, R., Surya Ulhas, R., Sudheer, W. N., Banadka, A., Nagella,P., … Almaghasla, M. I. (2023). The role of nanoparticles in response of plants to abiotic stress at physiological, biochemical, and molecular levels. Plants, 12(2), 292.
93. Keke L, Yiting L, Xiaohui Y, Yi Y, Junliang Y, Yunfeng C, Yongxing Z (2025) Silica nanoparticles enhanced seed germination and seedling growth of drought-stressed wheat by modulating antioxidant enzymes and mitigating lipid peroxidation. Environ Science: Nano 12(6):3231–3246
94. Ray, M. K., Mishra, A. K., Mohanta, Y. K., Mahanta, S., Chakrabartty, I., Kungwani,N. A., … Pudake, R. N. (2023). Nanotechnology as a promising tool against phytopathogens:a futuristic approach to agriculture. Agriculture, 13(9), 1856.

95. Sun, K., Pan, Y. T., Jiang, H. J., Xu, J. Y., Ma, C. Y., Zhou, J., … Dai, C. C. (2024).Root endophyte-mediated alteration in plant H2O2 homeostasis regulates symbiosis outcome and reshapes the rhizosphere microbiota. Journal of Experimental Botany, 75(10), 3153–3170.
96. Ji H, Yu K, Wang H, Yang H (2024) Nanoclay mediated self-promoted reactive oxygen species releasing enables efficient antimicrobial. Adv Funct Mater 34(45):2407875
97. Gupta P, Sharma V, Nagpal G (2025) A comprehensive review of nano clay: From development and applications to research opportunities. Environ Prog Sustain Energy, 44(6), e70055
98. Shabbir R, Javed T, Sun SR, Wang ZQ, Zhang W, Gao SJ, Wang QN (2026) Reactive oxygen species-(ROS) in plant defense: jack-of-all-trades. Crit Rev Biotechnol 46(1):152–160
99. Solankey SS (ed) (2025) Advances in research on potato production. Springer
100. Ahirwar NK, Pachaya JS (2024) Effects of Climate Change on the spread and severity of Potato Virus Y: an In-depth examination. Asian J Microbiol Biotechnol 9:39–59
101. Tessema L, Kakuhenzire R, Seid E, Tafesse S, Tadesse Y, Negash K, McEwan M (2024) Detection of six potato viruses using double antibody sandwich ELISA from in vitro, screen house and field grown potato crops in Ethiopia. Discover Appl Sci 6(3):79
102. Kumar R, Tiwari RK, Sundaresha S, Kaundal P, Raigond B (2022) Potato viruses and their management. Sustainable management of potato pests and diseases. Springer Singapore, Singapore, pp 309–335
103. Kumar R, Tiwari RK, Sundaresha S, Kaundal P, Raigond B (2022) Potato viruses and their management. Sustainable management of potato pests and diseases. Springer Singapore, Singapore, pp 309–335
104. Oueslati W, Meftah M (2026) Discriminating Adsorption, Hydration-State Transitions, and Ion Exchange During Cesium Retention on Montmorillonite: Implications for Mechanistic Understanding and Sorbent Design. Hybrid Adv, 100635
105. Bell MJ, Ransom MD, Thompson ML, Hinsinger P, Florence AM, Moody PW, Guppy CN (2020) Considering soil potassium pools with dissimilar plant availability. Improving potassium recommendations for agricultural crops. Springer International Publishing, Cham, pp 163–190
106. Mejri C, Oueslati W (2025) A Critical Review of Clay Minerals. *Groundwater Frontiers-Techniques Challenges: Techniques Challenges*
107. Sposito G (2008) The chemistry of soils. Oxford University Press
108. Junglee S, Urban L, Sallanon H, Lopez-Lauri F (2014) Optimized assay for hydrogen peroxide determination in plant tissue using potassium iodide. Am J Anal Chem 5(11):730
109. Angelini R, Manes F, Federico R (1990) Spatial and functional correlation between diamine-oxidase and peroxidase activities and their dependence upon de-etiolation and wounding in chickpea stems. Planta 182:89–96
110. CHO YK, AHN HK (1999) Purification and characterization of polyphenol oxidase from potato: II. Inhibition and catalytic mechanism. J Food Biochem 23(6):593–605
111. Sharma H, Sharma N (2025) A Review on the Efficient Release of Nutrients for Sustainable Agriculture. J Soil Sci Plant Nutr 25(3):7061–7073
112. Ray, A., Das, P., Chunduri, R., Kumar, D., Dulta, K., Kaushal, A., … Sharma, A. (2025).Nanocomposite-based agricultural delivery systems: a sustainable approach to enhanced crop productivity and soil health. Journal of Nanoparticle Research, 27(4), 110.
113. Noman, M., Ahmed, T., Ijaz, U., Hameed, A., Shahid, M., Azizullah, … Song, F. (2023).Microbe-oriented nanoparticles as phytomedicines for plant health management: an emerging paradigm to achieve global food security. Critical Reviews in Food Science and Nutrition, 63(25), 7489–7509.
114. Wang L, Pan T, Gao X, An J, Ning C, Li S, Cai K (2022) Silica nanoparticles activate defense responses by reducing reactive oxygen species under Ralstonia solanacearum infection in tomato plants. NanoImpact 28:100418
115. Kuć J, Shockley G, Kearney K (1975) Protection of cucumber against Colletotrichum lagenarium by Colletotrichum lagenarium. Physiol Plant Pathol 7(2):195–199
116. Torres MA, Jones JD, Dangl JL (2006) Reactive oxygen species signaling in response to pathogens. Plant Physiol 141(2):373–378
117. Passardi F, Cosio C, Penel C, Dunand C (2005) Peroxidases have more functions than a Swiss army knife. Plant Cell Rep 24(5):255–265

Figures

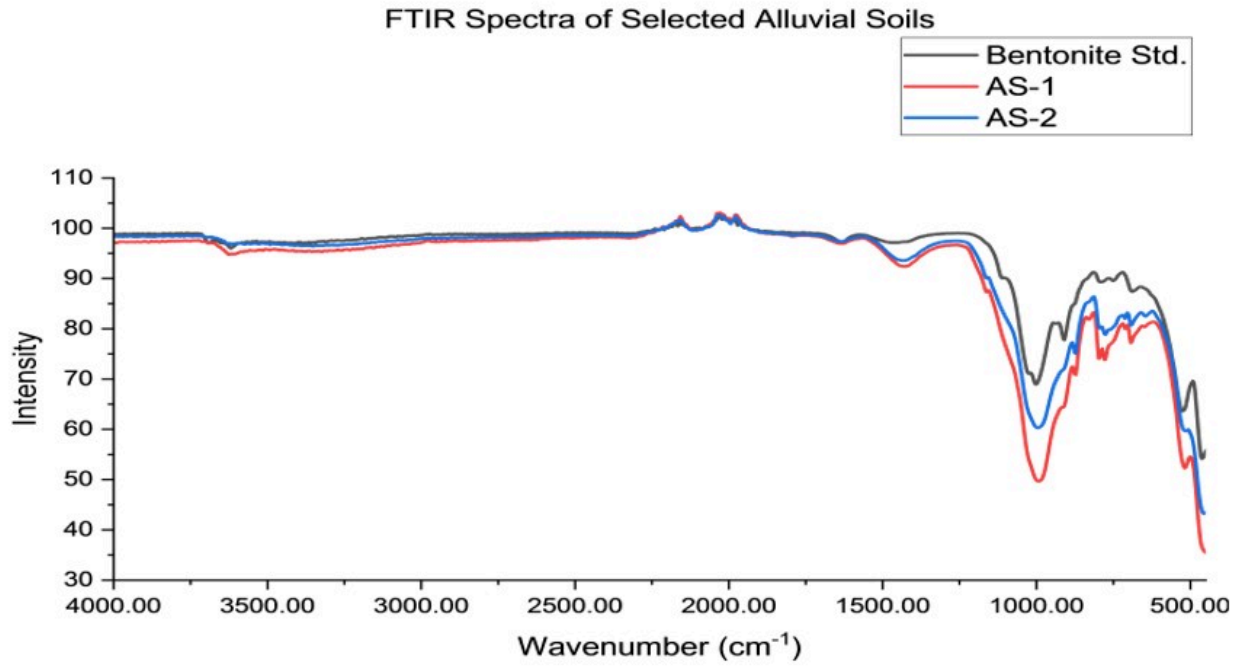


Figure 1

FTIR Analysis of Samples of Alluvial Deposits for Potential Bentonite

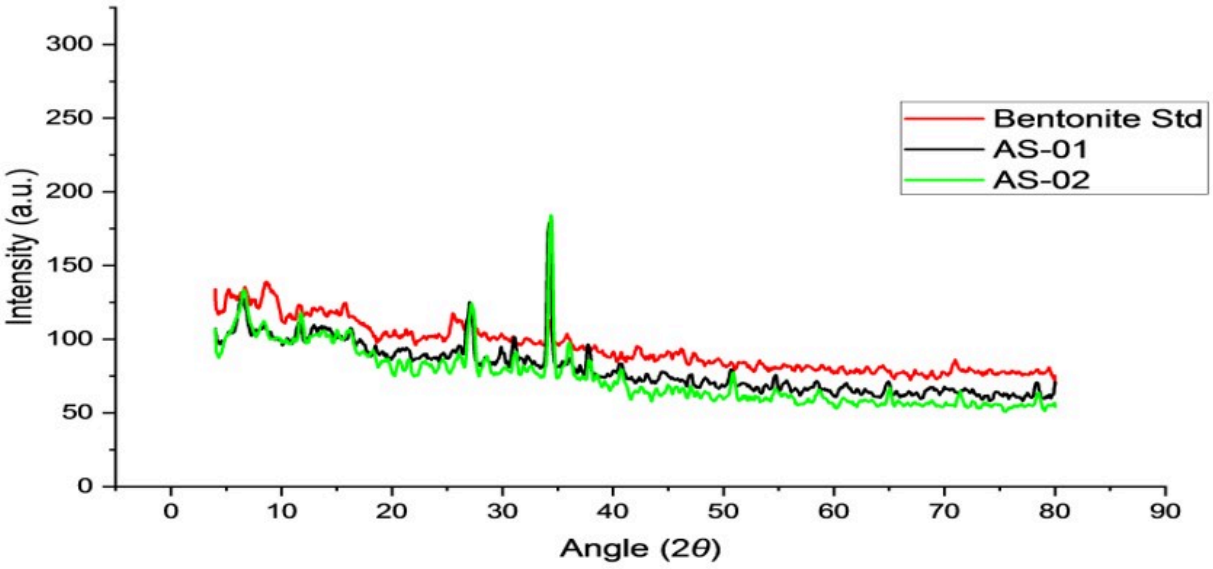


Figure 2

XRD Analysis of Samples of Alluvial Deposits for Potential Bentonite where AS-01 is the soil sample collected from Chirat Dam, AS-02 is the soil collected from Jalozai Sprin while Std Bentonite is the Bentonite procured from Sifviral load determined bygma Aldrich

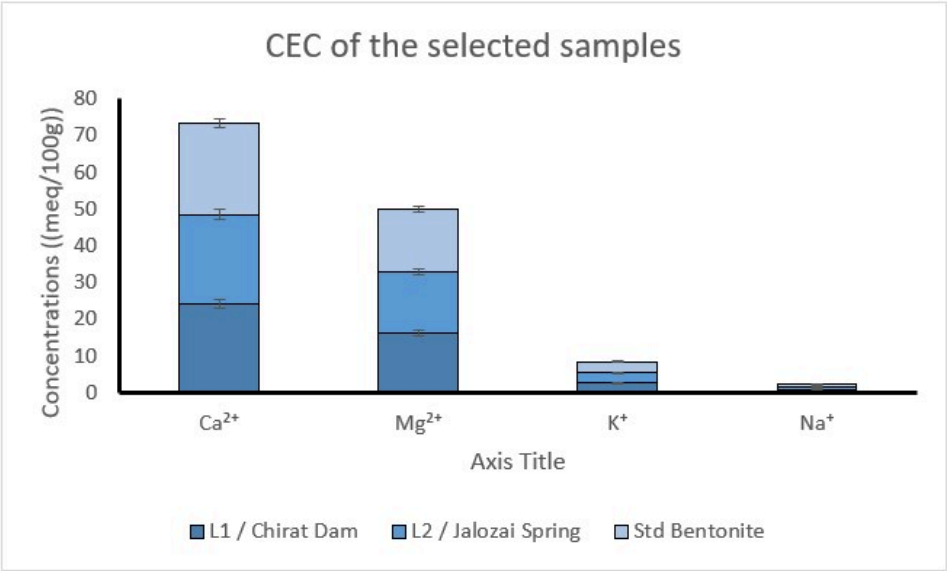


Figure 3

Cation Ion Exchange Capacity of Selected Samples